The $1 : \sqrt{2}$ mode interaction and heteroclinic networks in Boussinesq convection

Olga Podvigina[a−c] and Peter Ashwin[d]

[a]Observatoire de la Côte d'Azur, CNRS UMR 6529,
BP 4229, 06304 Nice Cedex 4, France
[b]International Institute of Earthquake Prediction Theory
and Mathematical Geophysics,
79 bldg. 2, Warshavskoe Ave., 113556 Moscow, Russian Federation
[c]Laboratory of General Aerodynamics, Institute of Mechanics,
Lomonosov Moscow State University,
1, Michurinsky Ave., 119899 Moscow, Russian Federation
[d]Mathematics Research Institute
University of Exeter
Exeter EX4 4QE, UK

June 28, 2007

Abstract

Methods of equivariant bifurcation theory are applied to Boussinesq convection in a plane layer with stress-free horizontal boundaries and an imposed square lattice periodicity in the horizontal directions. We consider the problem near the onset of instability of the uniform conducting state where spatial roll patterns with two different wavelengths in the ratio $1 : \sqrt{2}$ become simultaneously unstable at a mode interaction. Centre manifold reduction yields a normal form on $\mathbf{C}^4$ with very rich dynamical behavior. For a fixed Prandtl number P the mode interaction occurs at an isolated point in the parameter plane (R, L) (where R is the Rayleigh number and L the length of the horizontal periodicities) and acts as an organizing center for many nearby bifurcations. The normal form predicts appearance of many steady states and travelling waves, which are classified by their symmetries. It also predicts the appearance of robust heteroclinic networks involving steady states with several different symmetries, and robust attractors of generalized heteroclinic type that include connections from equilibria to subcycles. This is the first example of a heteroclinic network in a fluid dynamical system that has 'depth' greater than one. The normal form dynamics is in good correspondence (both quantitatively and qualitatively) with direct numerical simulations of the full convection equations.

Key words: mode interaction, steady-state bifurcation with symmetry, centre manifold reduction, Boussinesq convection, robust heteroclinic network

1   Introduction

Thermal convection, a common and important phenomenon in nature, is a subject of intensive scientific investigation for more than a century. It was investigated by a variety of analytical (asymptotic, perturbation, multiscale, etc.) and numerical methods, as well as by experimental work. Convection is a source of new ideas, for example, on pattern formation and on transition from order to chaos and from laminar to turbulent flows.

In this paper we consider fluid in a non-rotating plane horizontal layer heated from below, assuming Boussinesq approximation, whereby variation of density is neglected in the mass conservation equation and flows are regarded as incompressible. For small Rayleigh number, R, (proportional to the temperature difference between the horizontal boundaries) fluid is at rest and heat is transferred by thermal diffusion only. When R exceeds the critical value, fluid motion in the form of two-dimensional rolls sets in. We assume periodicity in horizontal directions with equal periods, such that instabilities with respect to rolls aligned along edges and along diagonals of the periodicity cell occur simultaneously (for the same value of R). Spatial periods of these critical modes are in the ratio $1 : \sqrt{2}$.

For a square periodicity cell the symmetry group of the system is $\mathbf{D}_4 \ltimes \mathbf{T}^2 \times \mathbf{Z}_2$ and the center eigenspace is $\mathbf{C}^4$. We derive a general third order ODE (a normal form) commuting with the action of the group on the center eigenspace, and study its bifurcations. The system has a large variety of steady states and travelling waves, which are classified by their symmetries. It can also possess heteroclinic connections forming complex networks. We derive sufficient conditions for existence of some of these connections.

Steady states emerging in a $\mathbf{D}_4 \ltimes \mathbf{T}^2 \times \mathbf{Z}_2$-symmetric system on $\mathbf{C}^2$ have been considered by a number of authors; notably [24, 21, 22], and bifurcations in a $\mathbf{D}_4 \ltimes \mathbf{T}^2$-symmetric system (to which equations of non-Boussinesq convection are reduced) involving $1 : \sqrt{2}$ mode interaction were studied in [20]. The Boussinesq case is richer, in particular, it gives rise to more steady states than found in [20]. We note that a number of other authors (e.g., [7, 6, 21, 22]) have considered related bifurcations to planforms for periodic boundary conditions on a square lattice.

We apply our results on bifurcations in the general normal form to the particular case of Boussinesq convection, considering the normal form for the values of coefficients calculated by the center manifold reduction of the equations of convection. We obtain bifurcation diagrams of the behavior near the mode interaction in terms of three parameters that generically unfold the problem, which are the Rayleigh number R, the domain size L and the Prandtl number P. We study attractors of the reduced system when the growth rates of roll modes (depending on R and L) are varied and P is fixed. This study was performed for several values of Prandtl number.

In addition to steady states and periodic orbits, the system possesses several types of heteroclinic attractor, as well as robust heteroclinic-type attractors incorporating connections between equilibria and sub-cycles. The latter are heteroclinic networks of 'depth two' in the terminology of [1], because there are trajectories within the attractor that connect unstable equilibria and heteroclinic cycles of the more conventional type. More precisely, there are connections that do not lie within the stable manifold of any relative equilibrium. Although such attractors have been found in other systems (e.g., replicator systems [4]) this is the first example in a dynamical system related to hydrodynamics.

Bifurcations of the normal form are compared with those observed in numerical simulations of equations of convection. Attractors in the systems are similar, and the critical values of parameters agree well.

2 Thermal convection in a plane layer

Consider the nondimensional equations for Boussinesq convection of a unit density fluid in a plane layer (x, y, z) (where $0 < z < 1$) uniformly heated from below. The flow velocity $\mathbf{v}$ and pressure p satisfy the Navier-Stokes equation

$$\frac{\partial \mathbf{v}}{\partial t} = \mathbf{v} \times (\nabla \times \mathbf{v}) + P\Delta \mathbf{v} + PR\theta \mathbf{e}_z - \nabla p \tag{1}$$

with incompressibility condition

$$\nabla \cdot \mathbf{v} = 0. \tag{2}$$

The heat transfer equation

$$\frac{\partial \theta}{\partial t} = -(\mathbf{v} \cdot \nabla)\theta + v_z + \Delta \theta \tag{3}$$

gives the evolution of θ, the difference between the temperature in the flow and the linear temperature profile. The parameters R and P are the Rayleigh and Prandtl numbers, respectively. We assume stress-free boundary conditions for the flow and fixed temperature on horizontal boundaries:

$$\frac{\partial v_x}{\partial z} = \frac{\partial v_y}{\partial z} = v_z = 0, \qquad \theta = 0 \qquad \text{at } z = 0, 1. \tag{4}$$

For the remainder of the paper we will consider only those flows that are periodic on a square lattice in the (x, y)-plane, i.e. such that there is an $L > 0$ such that

$$\mathbf{v}(x, y, z) = \mathbf{v}(x + pL, y + qL, z) \quad \text{and} \quad \theta(x, y, z) = \theta(x + pL, y + qL, z) \tag{5}$$

for any $(p, q) \in \mathbf{Z}^2$.

The system Eq. (1-4) admits the trivial solution $\mathbf{v} = 0$, $\theta = 0$ describing pure thermal conduction. The steady state becomes unstable to perturbations with wavenumber k at $R = (k^2 + \pi^2)^3 k^{-2}$ with an associated eigenvector

$$\mathbf{V}(k) = \begin{pmatrix} -\pi k^{-1} \cos \pi z \sin kx \\ 0 \\ \sin \pi z \cos kx \\ (k^2 + \pi^2)^{-1} \sin \pi z \cos kx \end{pmatrix}. \tag{6}$$

(Other eigenvectors can be obtained by application of symmetries of the system.) The critical Rayleigh number for the onset of convection is $R = \frac{27}{4}\pi^4 \approx 657$, and the critical wavenumber is $k_c = \pi/\sqrt{2}$. Figure 1 shows the instability neutral curves for the first few modes in the (k, R) plane.

Modes with wavenumbers k and $\sqrt{2}k$ become unstable simultaneously at

$$R_m = 2^{-2/3}(2^{1/3} + 1)^{-2}(2^{2/3} + 2^{1/3} + 1)^3 \pi^4 \approx 684 \tag{7}$$

while the critical wavenumber for the mode interaction point satisfies

$$k_m = 2^{-1/6}(2^{1/3} + 1)^{-1/2}\pi \approx 1.86 \tag{8}$$

in agreement with the value reported in [20]. The periodicity L in Eq. (5) is chosen to be close to the critical value

$$L_m = 2\pi/k_m = 2 \cdot 2^{1/6}(2^{1/3} + 1)^{1/2} \tag{9}$$

so that the rolls $\mathbf{V}(k_m)$ are aligned along the edges of the periodicity cell. The rolls

$$\mathbf{W}(k_m) = \begin{pmatrix} -\pi k_m^{-1} \cos \pi z \sin(k_m x + k_m y) \\ -\pi k_m^{-1} \cos \pi z \sin(k_m x + k_m y) \\ \sin \pi z \cos(k_m x + k_m y) \\ (2k_m^2 + \pi^2)^{-1} \sin \pi z \cos(k_m x + k_m y) \end{pmatrix} \tag{10}$$

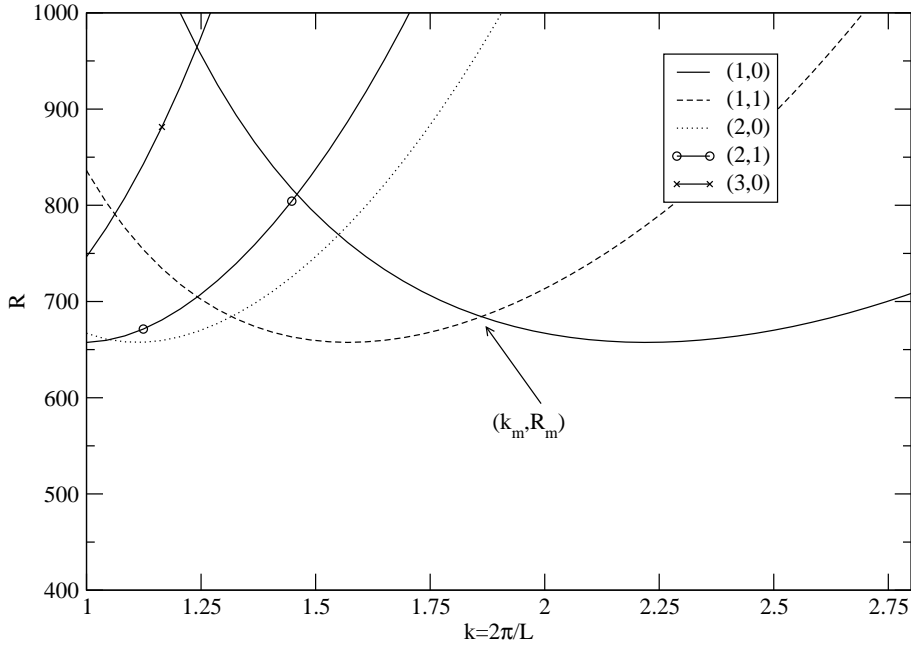with the wavenumber $\sqrt{2}k_m$ are aligned along a diagonal.

3

Figure 1: *Critical Rayleigh number R as a function of $k = 2\pi/L$ for a range of modes in a box with horizontal dimension L. The line (p, q) indicates where the trivial steady state $\mathbf{v} = \mathbf{0}$ $\theta = 0$ becomes unstable to the mode with wavevector (pk, qk, π); there are additional lines for lower k and higher $p^2 + q^2$ that accumulate on $k = 0$. The point (k_m, R_m) shows where the $1 : \sqrt{2}$ mode interaction occurs.*

2.1   The symmetry group

The symmetry group of the convective system Eq. (1-3) with the boundary conditions Eq. (4,5) can be expressed as $\mathbf{D}_4 \ltimes \mathbf{T}^2 \times \mathbf{Z}_2$. The 8-element group of symmetries of the square lattice, $\mathbf{D}_4$, is comprised of the set of rotations

$$s_1 : \ (x, y, z) \mapsto (y, -x, z),$$

$$s_2 : \ (x, y, z) \mapsto (-x, -y, z),$$

$$s_3 : \ (x, y, z) \mapsto (-y, x, z),$$

reflections

$$s_4 : \ (x, y, z) \mapsto (x, -y, z),$$

$$s_5 : \ (x, y, z) \mapsto (-x, y, z),$$

$$s_6 : \ (x, y, z) \mapsto (y, x, z),$$

$$s_7 : \ (x, y, z) \mapsto (-y, -x, z)$$

and the identity $s_0 = e$. The group $\mathbf{T}^2 = \mathbf{T}_x \times \mathbf{T}_y$ where $\mathbf{T}_x$ and $\mathbf{T}_y$ are groups of translations in the x and y directions, respectively:

$$\gamma_\alpha^x : \ (x, y, z) \mapsto (x + \alpha, y, z)$$

and

$$\gamma_\alpha^y : \ (x, y, z) \mapsto (x, y + \alpha, z)$$

where $0 \le \alpha < L$ (so that $\gamma_L^x = \gamma_L^y = e$). Denote by $\mathbf{T}_{xy}$ the group of translations along the diagonal:

$$\gamma_\alpha^{xy} : \ (x, y, z) \mapsto (x + \alpha, y + \alpha, z).$$

4

The group $\mathbf{Z}_2$ is generated by the so-called Boussinesq symmetry, which is reflection about the horizontal midplane:

$$r : \ (x, y, z) \mapsto (x, y, 1 - z).$$

Consider a centre eigenspace spanned by rolls Eq. (6,10) and their symmetric images

$$
\begin{aligned}
\mathbf{X}_1 &= \mathbf{V}, \quad \mathbf{Y}_1 = \gamma^x_{L/4}\mathbf{V}, \quad \mathbf{X}_2 = s_6\mathbf{V}, \quad \mathbf{Y}_2 = \gamma^y_{L/4}s_6\mathbf{V}, \\
\mathbf{X}_3 &= \mathbf{W}, \quad \mathbf{Y}_3 = \gamma^x_{L/4}\mathbf{W}, \quad \mathbf{X}_4 = s_4\mathbf{W} \text{ and } \mathbf{Y}_4 = \gamma^x_{L/4}s_4\mathbf{W}.
\end{aligned}
\tag{11}
$$

The coordinates $(z_1, z_2, z_3, z_4) \in \mathbf{C}^4$ on the center manifold can be introduced as projections in the directions $\mathbf{X}_j$ and $\mathbf{Y}_j$, $j = 1, 2, 3, 4$. The symmetries of the system transform the coordinates in the following way:

$$
\begin{aligned}
s_1 &: \ (z_1, z_2, z_3, z_4) &\mapsto& \ (z_2, \bar{z}_1, \bar{z}_4, z_3), \\
s_2 &: \ (z_1, z_2, z_3, z_4) &\mapsto& \ (\bar{z}_1, \bar{z}_2, \bar{z}_3, \bar{z}_4), \\
s_3 &: \ (z_1, z_2, z_3, z_4) &\mapsto& \ (\bar{z}_2, z_1, z_4, \bar{z}_3), \\
s_4 &: \ (z_1, z_2, z_3, z_4) &\mapsto& \ (z_1, \bar{z}_2, z_4, z_3), \\
s_5 &: \ (z_1, z_2, z_3, z_4) &\mapsto& \ (\bar{z}_1, z_2, \bar{z}_4, \bar{z}_3), \\
s_6 &: \ (z_1, z_2, z_3, z_4) &\mapsto& \ (z_2, z_1, z_3, \bar{z}_4), \\
s_7 &: \ (z_1, z_2, z_3, z_4) &\mapsto& \ (\bar{z}_2, \bar{z}_1, \bar{z}_3, z_4), \\
\gamma^x_\alpha &: \ (z_1, z_2, z_3, z_4) &\mapsto& \ (e^{2\pi i\alpha/L}z_1, z_2, e^{2\pi i\alpha/L}z_3, e^{2\pi i\alpha/L}z_4), \\
\gamma^y_\alpha &: \ (z_1, z_2, z_3, z_4) &\mapsto& \ (z_1, e^{2\pi i\alpha/L}z_2, e^{2\pi i\alpha/L}z_3, e^{-2\pi i\alpha/L}z_4). \\
r &: (z_1, z_2, z_3, z_4) &\mapsto& \ (-z_1, -z_2, -z_3, -z_4).
\end{aligned}
$$

2.2 Normal form

The normal form on centre manifold $\mathbf{C}^4$ for the symmetry group $\mathbf{D}_4 \ltimes \mathbf{T}^2$ was considered by [20]. In the presence of the Boussinesq symmetry, the even order terms vanish meaning that the normal form with $\mathbf{D}_4 \ltimes \mathbf{T}^2 \times \mathbf{Z}_2$ symmetry truncated at cubic order is:

$$
\begin{aligned}
\dot{z}_1 &= \lambda_1 z_1 + z_1(A_1|z_1|^2 + A_2|z_2|^2 + A_3(|z_3|^2 + |z_4|^2)) + A_4\bar{z}_1 z_3 z_4, \\
\dot{z}_2 &= \lambda_1 z_2 + z_2(A_1|z_2|^2 + A_2|z_1|^2 + A_3(|z_3|^2 + |z_4|^2)) + A_4\bar{z}_2 z_3 \bar{z}_4, \\
\dot{z}_3 &= \lambda_2 z_3 + z_3(A_5|z_3|^2 + A_6|z_4|^2 + A_7(|z_1|^2 + |z_2|^2)) + A_8(z_2^2 z_4 + z_1^2\bar{z}_4), \\
\dot{z}_4 &= \lambda_2 z_4 + z_4(A_5|z_4|^2 + A_6|z_3|^2 + A_7(|z_1|^2 + |z_2|^2)) + A_8(\bar{z}_2^2 z_3 + z_1^2\bar{z}_3),
\end{aligned}
\tag{12}
$$

where A_i are real numbers (the normal form coefficients). The linear growth rates λ_1 and λ_2 are close to zero for the truncation to be valid; otherwise higher order terms become important. In Section 4 we relate λ_i and A_i to the Boussinesq problem for parameters (k, R) close to (k_m, R_m) (implying that L is close to L_m).

In polar coordinates $z_j = r_j e^{i\theta_j}$ (with $r_j \geq 0$ and $\theta_j \in [0, 2\pi)$) the normal form becomes:

$$
\begin{aligned}
\dot{r}_1 &= r_1(\lambda_1 + A_1 r_1^2 + A_2 r_2^2 + A_3(r_3^2 + r_4^2)) + A_4 r_1 r_3 r_4 \cos(\theta_4 + \theta_3 - 2\theta_1) \\
\dot{r}_2 &= r_2(\lambda_1 + A_1 r_2^2 + A_2 r_1^2 + A_3(r_3^2 + r_4^2)) + A_4 r_2 r_3 r_4 \cos(\theta_3 - 2\theta_2 - \theta_4) \\
\dot{r}_3 &= r_3(\lambda_2 + A_5 r_3^2 + A_6 r_4^2 + A_7(r_1^2 + r_2^2)) \\
&\quad + A_8(r_2^2 r_4 \cos(2\theta_2 + \theta_4 - \theta_3) + r_1^2 r_4 \cos(2\theta_1 - \theta_4 - \theta_3)) \\
\dot{r}_4 &= r_4(\lambda_2 + A_5 r_4^2 + A_6 r_3^2 + A_7(r_1^2 + r_2^2)) \\
&\quad + A_8(r_2^2 r_3 \cos(\theta_3 - 2\theta_2 - \theta_4) + r_1^2 r_3 \cos(2\theta_1 - \theta_3 - \theta_4)) \\
\dot{\theta}_1 &= A_4 r_3 r_4 \sin(\theta_3 + \theta_4 - 2\theta_1) \\
\dot{\theta}_2 &= A_4 r_3 r_4 \sin(\theta_3 - 2\theta_2 - \theta_4) \\
r_3 \dot{\theta}_3 &= A_8(r_2^2 r_4 \sin(2\theta_2 + \theta_4 - \theta_3) + r_1^2 r_4 \sin(2\theta_1 - \theta_4 - \theta_3)) \\
r_4 \dot{\theta}_4 &= A_8(r_2^2 r_3 \sin(\theta_3 - 2\theta_2 - \theta_4) + r_1^2 r_3 \sin(2\theta_1 - \theta_3 - \theta_4))
\end{aligned}
\tag{13}
$$

The expressions in the r.h.s. of Eq. (13) involve angles only in the following combinations: $\phi = 2\theta_1 - \theta_3 - \theta_4$ and $\psi = 2\theta_2 - \theta_3 + \theta_4$, and a pattern with constant r_j, $j = 1, 2, 3, 4$, can be described by the coordinates $(r_1, r_2, r_3, r_4, \phi, \psi)$. Note that relative equilibria for Eq. (12) are solutions of Eq. (13) with $\dot{r}_j = 0$ constant. These drift on the group orbit if either $\phi \neq 0 (\mathrm{mod}\,\pi)$ or $\psi \neq 0 (\mathrm{mod}\,\pi)$. Below we use the 6-dimensional polar coordinates $(\mathbf{r}, \phi, \psi)$ as well as the 4-dimensional complex Cartesian coordinates $\mathbf{z}$.

3 Bifurcations of the normal form Eq. (12) for a general set of coefficients

First we consider the solutions and bifurcation structure for generic choice of the real normal form coefficients A_i, $i = 1, \cdots, 8$. We define the primary bifurcations to be bifurcations of the trivial (non-convecting) state $(0, 0, 0, 0)$; this creates primary branches of solutions. A bifurcation from a primary branch is called a secondary bifurcation and creates secondary branches and similarly a bifurcation from secondary branches is a tertiary bifurcation and creates tertiary branches. In the case that a branch starts at a primary branch and ends at a secondary branch referred to as tertiary. We study bifurcations occurring when λ_i are varied and A_j are fixed: for convection (see Section 5) this corresponds to a fixed P and a varying R and L. Generic bifurcations of equilibria of different symmetry types occurring in the normal form (12) are summarized in Figure 2 and the structure of emerging steady states and travelling waves is illustrated in Figure 3.

For the action of $\mathbf{D}_4 \ltimes \mathbf{T}^2 \times \mathbf{Z}_2$ on $\mathbf{C}_4$ we consider, steady states with symmetry groups not listed in Figure 2 can exist, for example $(x_1, x_2, 0, 0)$, $(0, 0, x_3, x_4)$ and (x_1, x_2, x_3, x_3), although these are not isolated solutions for the normal form Eq. (12). In fact the third order normal form is degenerate and to resolve the degeneracy some of the fifth order terms should be included. (See e.g. the study of bifurcations in a $\mathbf{D}_4$-symmetric system on $\mathbf{R}^2$ in [9]). However, these solutions emerge only in the special cases $A_1 - A_2 = 0$ or $A_5 - A_6 = 0$. For the considered convective system in fact these differences are always positive (see Section 4), meaning that the third order truncation is sufficient.

3.1 Primary bifurcations

Bifurcations from the trivial steady state S_0, $(z_1, z_2, z_3, z_4) = \mathbf{0}$, take place when $\lambda_1 = 0$ or $\lambda_2 = 0$. In both subspaces the group action is isomorphic to $\mathbf{D}_4 \ltimes \mathbf{T}^2$, therefore branches of steady states listed in Table 1 can be obtained applying standard results.
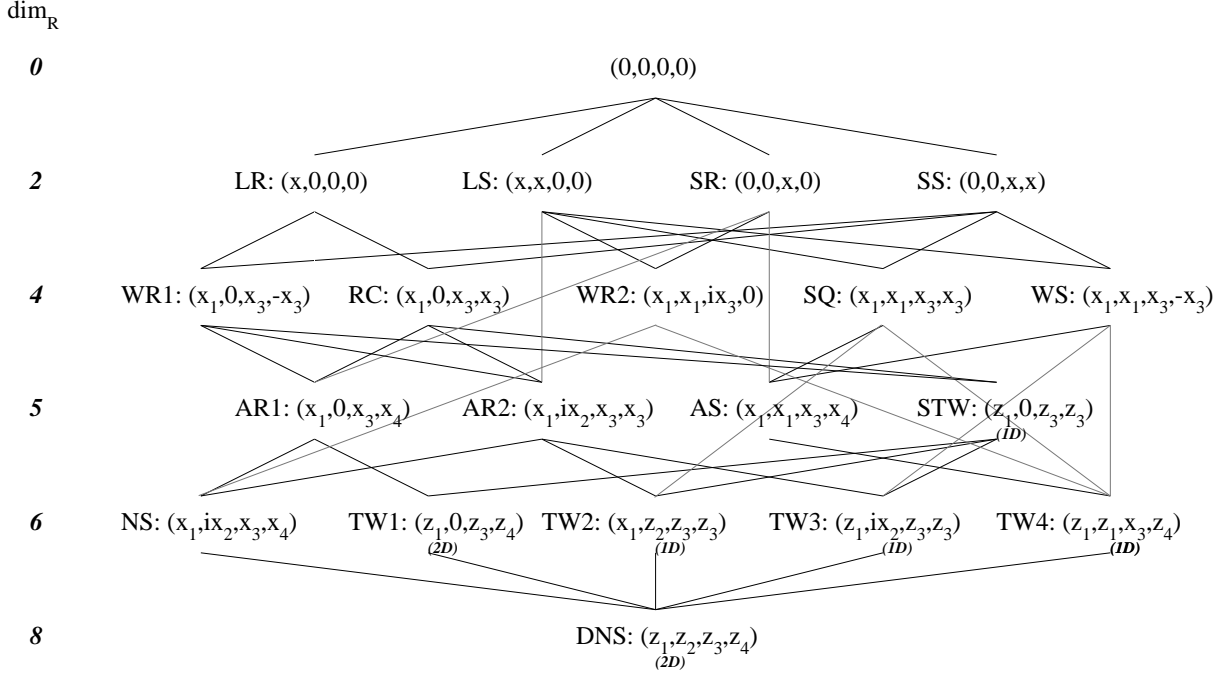
dim$_R$

0 $(0,0,0,0)$

2 LR: $(x,0,0,0)$ LS: $(x,x,0,0)$ SR: $(0,0,x,0)$ SS: $(0,0,x,x)$

4 WR1: $(x_1,0,x_3,-x_3)$ RC: $(x_1,0,x_3,x_3)$ WR2: $(x_1,x_1,ix_3,0)$ SQ: (x_1,x_1,x_3,x_3) WS: $(x_1,x_1,x_3,-x_3)$

5 AR1: $(x_1,0,x_3,x_4)$ AR2: (x_1,ix_2,x_3,x_3) AS: (x_1,x_1,x_3,x_4) STW: $(z_1,0,z_3,z_3)$
(1D)

6 NS: (x_1,ix_2,x_3,x_4) TW1: $(z_1,0,z_3,z_4)$ TW2: (x_1,z_2,z_3,z_3) TW3: (z_1,ix_2,z_3,z_3) TW4: (z_1,z_1,x_3,z_4)
(2D)   *(1D)*   *(1D)*   *(1D)*

8 DNS: (z_1,z_2,z_3,z_4)
(2D)

Figure 2: *Lattice of symmetry types of relative equilibria emerging in the normal form (12). The dimensions of the group orbits of these states are shown on the left, and the generic dimension of drift of the drifting states STW, TW1, TW2, TW3, TW4 and DNS (drifting no symmetry) are shown.*

Bifurcates at	Name	Group	Generators	Typical point	Amplitude	No
$\lambda_1 = 0$	LR	$\mathbf{D}_2 \ltimes \mathbf{T} \times \mathbf{Z}_2$	$s_2, s_4, \gamma_\alpha^y, \gamma_{L/2}^x r$	$(x,0,0,0)$	$x^2 = -\lambda_1/A_1$	$1, 29$
$\lambda_1 = 0$	LS	$\mathbf{D}_4 \times \mathbf{Z}_2$	$s_1, s_4, \gamma_{L/2}^{xy} r$	$(x,x,0,0)$	$x^2 = -\lambda_1/(A_1 + A_2)$	$1, 29$
$\lambda_2 = 0$	SR	$\mathbf{D}_2 \ltimes \mathbf{T} \ltimes \mathbf{Z}_4$	$s_2, s_6, \gamma_\alpha^{x,-y}, \gamma_{L/4}^{xy} r$	$(0,0,x,0)$	$x^2 = -\lambda_2/A_5$	$2, 33$
$\lambda_2 = 0$	SS	$\mathbf{D}_4 \ltimes \mathbf{Z}_2$	$s_1, s_4, \gamma_{L/2}^x r$	$(0,0,x,x)$	$x^2 = -\lambda_2/(A_5 + A_6)$	$2, 33$

Table 1: *Steady state branches bifurcating from S_0: the condition for occurrence of the bifurcation, label of the bifurcating steady state, the symmetry group of the state, generators of the group, typical point and equation for the branch. The last column gives the bifurcation numbers in the order of reference in sections 4, 5 and 6.*
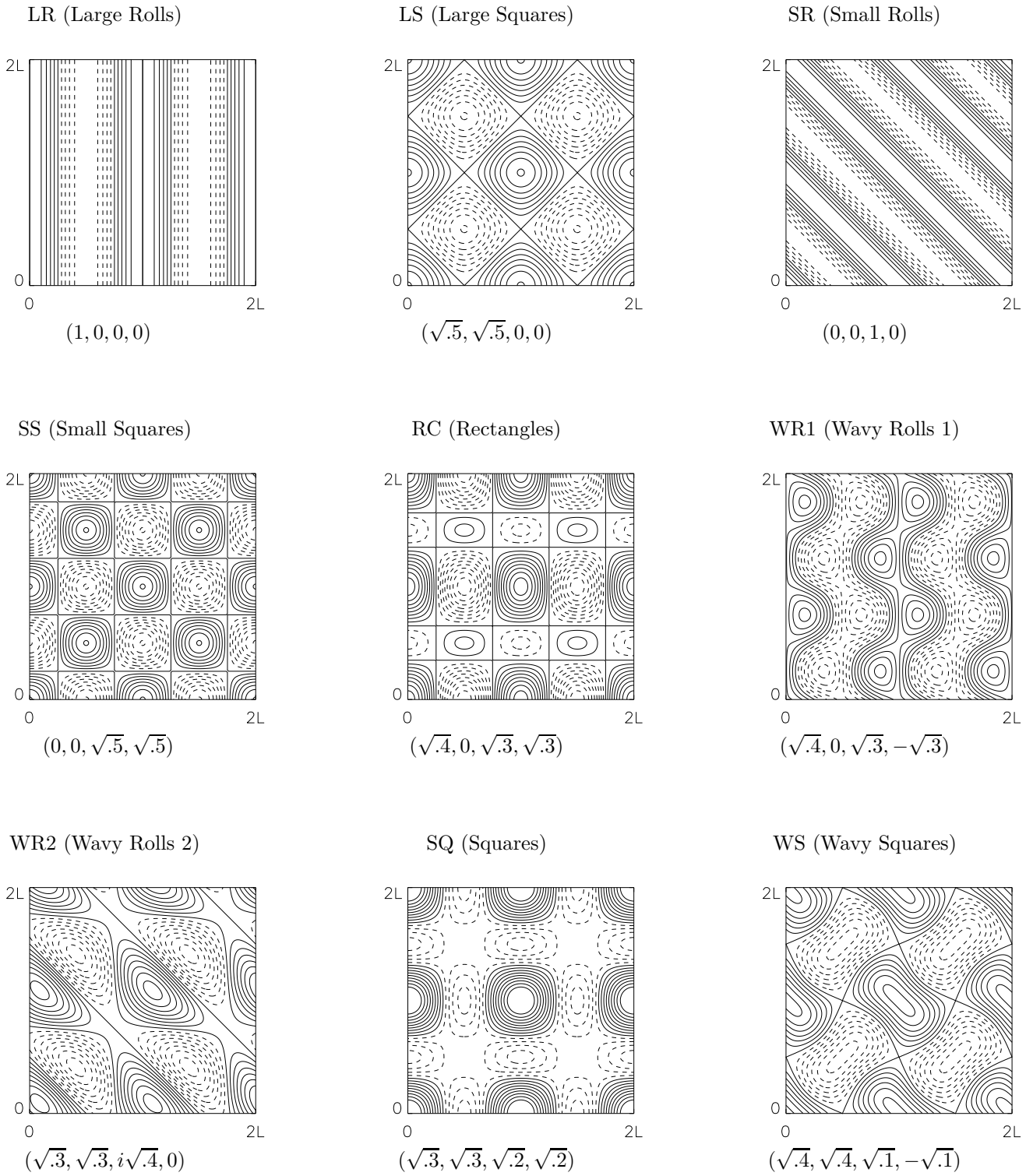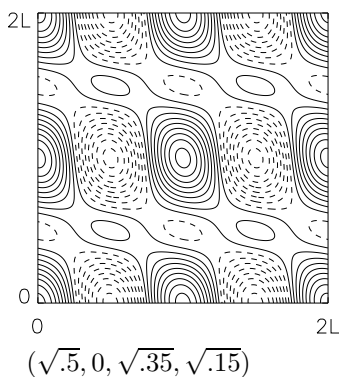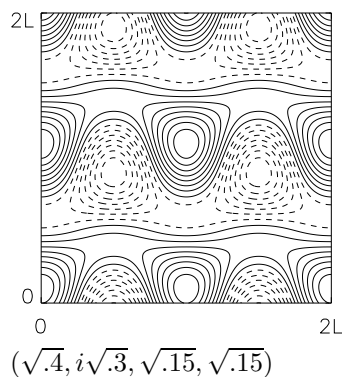
LR (Large Rolls)   LS (Large Squares)   SR (Small Rolls)

$(1, 0, 0, 0)$ $(\sqrt{.5}, \sqrt{.5}, 0, 0)$ $(0, 0, 1, 0)$

SS (Small Squares)   RC (Rectangles)   WR1 (Wavy Rolls 1)

$(0, 0, \sqrt{.5}, \sqrt{.5})$ $(\sqrt{.4}, 0, \sqrt{.3}, \sqrt{.3})$ $(\sqrt{.4}, 0, \sqrt{.3}, -\sqrt{.3})$

WR2 (Wavy Rolls 2)   SQ (Squares)   WS (Wavy Squares)

$(\sqrt{.3}, \sqrt{.3}, i\sqrt{.4}, 0)$ $(\sqrt{.3}, \sqrt{.3}, \sqrt{.2}, \sqrt{.2})$ $(\sqrt{.4}, \sqrt{.4}, \sqrt{.1}, -\sqrt{.1})$

Figure 3: *Isolines (step 0.2) of the vertical component of the velocity in the horizontal midplane for convective steady states and travelling waves evaluated for the respective solutions of Eq. (12). Four copies of the periodicity cell is shown for clarity. The relation between convective and solutions of Eq. (12) is given by Eq. (6), Eq. (10) and Eq. (11). The numbers below a pattern are coordinates of the pattern on the center manifold in the basis defined by Eq. (11).*

8

AR1 (Asymm. Rolls 1)

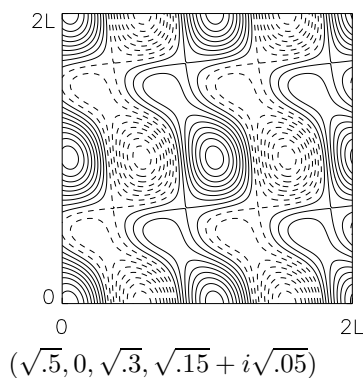$(\sqrt{.5}, 0, \sqrt{.35}, \sqrt{.15})$

AR2 (Asymm. Rolls 2)

$(\sqrt{.4}, i\sqrt{.3}, \sqrt{.15}, \sqrt{.15})$

AS (Asymm. Squares)

$(\sqrt{.3}, \sqrt{.3}, \sqrt{.25}, \sqrt{.15})$
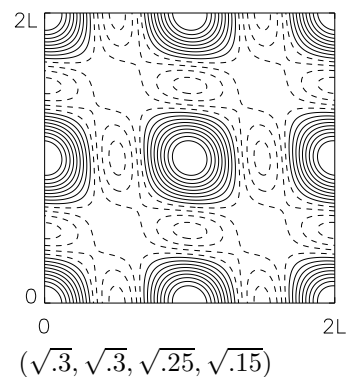
STW (Symm. Travelling Waves)

$(\sqrt{.4}, 0, \sqrt{.2} + i\sqrt{.1}, \sqrt{.2} + i\sqrt{.1})$
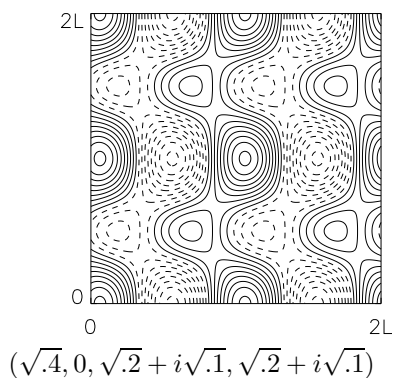
TW1 (Travelling Waves 1)

$(\sqrt{.5}, 0, \sqrt{.3}, \sqrt{.15} + i\sqrt{.05})$

TW2 (Travelling Waves 2)

$(\sqrt{.4}, \sqrt{.2}, \sqrt{.15} + i\sqrt{.05}, \sqrt{.15} + i\sqrt{.05})$
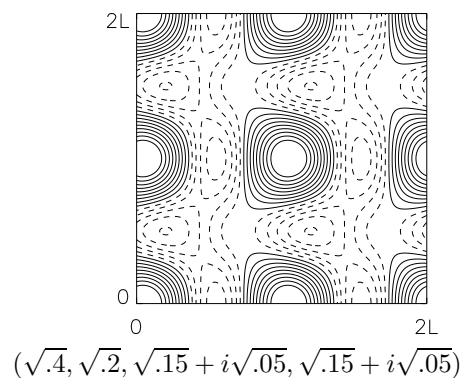
TW3 (Travelling Waves 3)

$(\sqrt{.4}, \sqrt{.2}, \sqrt{.15} + i\sqrt{.05}, -\sqrt{.15} - i\sqrt{.05})$
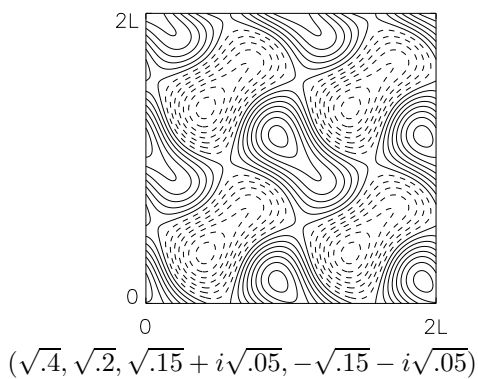
TW4 (Travelling Waves 4)

$(\sqrt{.3}, \sqrt{.3}, \sqrt{.2} + i\sqrt{.05}, \sqrt{.15})$
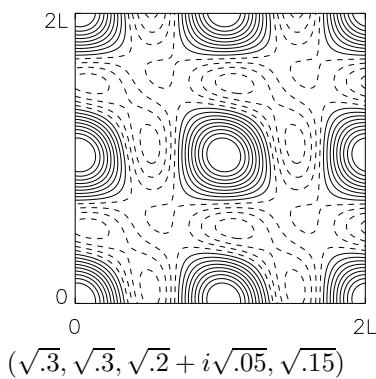
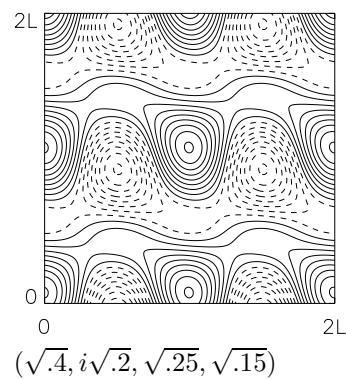NS (Nonsymmetric Steady)

$(\sqrt{.4}, i\sqrt{.2}, \sqrt{.25}, \sqrt{.15})$

Figure 3 continued

9

Steady state	Typical point	Invariant subspaces	Eigenvalues	Action	Kernel
LR	$(x,0,0,0)$	$(q,0,0,0)$	$-2\lambda_1$	$\mathbf{1}$	all
		$(iq,0,0,0)$	0	$\mathbf{Z}_2$	$s_4, \gamma_\alpha^y, \gamma_{L/2}^x r$
		$(0,w,0,0)$	$\lambda_1(A_1-A_2)/A_1$	$\mathbf{Z}_2 \ltimes \mathbf{T}$	$\gamma_{L/2}^{xy} r, s_5$
		$(0,0,w,\bar{w})$	$\lambda_2+(A_7+A_8)x^2$	$\mathbf{Z}_2 \ltimes \mathbf{T}$	$s_5, \gamma_{L/2}^x r$
		$(0,0,w,-\bar{w})$	$\lambda_2+(A_7-A_8)x^2$	$\mathbf{Z}_2 \ltimes \mathbf{T}$	$\gamma_{L/2}^x r, \gamma_{L/2}^y s_5$
LS	$(x,x,0,0)$	$(q,q,0,0)$	$-2\lambda_1$	$\mathbf{1}$	all
		$(iq_1,iq_2,0,0)$	0	$\mathbf{D}_4$	$\gamma_{L/2}^{xy} r$
		$(q,-q,0,0)$	$2\lambda_1(A_2-A_1)/(A_1+A_2)$	$\mathbf{Z}_2$	$s_2, s_4, \gamma_{L/2}^{xy} r$
		$(0,0,q,q)$	$\lambda_2+2(A_7+A_8)x^2$	$\mathbf{Z}_2$	s_1, s_4
		$(0,0,q,-q)$	$\lambda_2+2(A_7-A_8)x^2$	$\mathbf{Z}_2$	$s_2, \gamma_{L/2}^{xy} r s_1$
		$(0,0,iq_1,iq_2)$	$\lambda_2+2A_7 x^2$	$\mathbf{D}_4$	$\gamma_{L/2}^{xy} r s_2$
SR	$(0,0,x,0)$	$(0,0,q,0)$	$-2\lambda_2$	$\mathbf{1}$	all
		$(0,0,iq,0)$	0	$\mathbf{Z}_2$	$s_6, \gamma_\alpha^{x,-y}, \gamma_{L/4}^{xy} r$
		$(0,0,0,w)$	$\lambda_2(A_5-A_6)/A_5$	$\mathbf{Z}_2 \ltimes \mathbf{T}$	$s_7, \gamma_{L/2}^x r$
		$(w_1,w_2,0,0)$	$\lambda_1+A_3 x^2$	$\mathbf{D}_2 \ltimes \mathbf{T} \times \mathbf{Z}_4$	
SS	$(0,0,x,x)$	$(0,0,q,q)$	$-2\lambda_2$	$\mathbf{1}$	all
		$(0,0,iq_1,iq_2)$	0	$\mathbf{D}_4$	$\gamma_{L/2}^x r$
		$(0,0,q,-q)$	$2\lambda_2(A_6-A_5)/(A_5+A_6)$	$\mathbf{Z}_2$	$s_2, s_6, \gamma_{L/2}^x r$
		$(q_1,q_2,0,0)$	$\lambda_1+(2A_3+A_4)x^2$	$\mathbf{D}_4$	s_2, s_4
		$(iq_1,iq_2,0,0)$	$\lambda_1+(2A_3-A_4)x^2$	$\mathbf{D}_4$	$s_4\gamma_{L/2}^x r, s_5\gamma_{L/2}^y r$

Table 2: *Invariant subspaces and associated eigenvalues that determine the stability of respective steady states. The fifth column gives the action of the steady state symmetry groups on the subspace and the sixth column gives the generators of the kernel of this action.*

3.2 Secondary bifurcations

In this subsection we study bifurcations from the primary steady states. To label the bifurcating branches we try to follow the terminology used in [20] as much as possible, however, in our case there are more types of steady state because of the presence of the Boussinesq symmetry.

Table 2 presents eigenspaces and associated eigenvalues of the mapping Eq. (12) linearized in the vicinity of the respective steady states. The fifth column gives the action of the steady state symmetry groups on the eigenspaces, and the sixth column indicates which elements of this group act trivially.

Bifurcation takes places if an eigenvalue crosses the imaginary axis. From the action of the symmetry group on the associated eigenspace we determine branches of bifurcating solutions, using results [9] for the respective group. Bifurcations from primary branches are listed in Table 3. Branching equations can be obtained by substitution of expressions for steady states into Eq. (12); they are cumbersome and not listed here. We did not find in the literature any analysis of bifurcations with the symmetry group $\mathbf{D}_2 \ltimes \mathbf{T} \times \mathbf{Z}_4$ (from SR); hence we include branching and the stability conditions for the branches for this group as Appendix A.

3.3 Tertiary bifurcations

In this subsection we consider stability and bifurcation of secondary steady states, i.e. those connecting branches of primary steady states. They have symmetry groups isomorphic to $\mathbf{D}_4$, $\mathbf{D}_2 \times \mathbf{Z}_2$ or to $\mathbf{D}_2$. Similarly to above, to determine stability we decompose $\mathbf{C}^4$ into isotypic components for the action of the groups and calculate the eigenvalues of the linearization of Eq. (12) near the steady state,

Bifurcates at	Name	Group	Generators	Typical point	No
FROM LR=$(x,0,0,0)$					
$\lambda_2 + (A_7+A_8)x^2 = 0$	RC	$\mathbf{D}_2 \times \mathbf{Z}_2$	$s_2, s_5, \gamma_{L/2}^x r$	$(x_1,0,x_3,x_3)$	17
$\lambda_2 + (A_7-A_8)x^2 = 0$	$WR1$	$\mathbf{D}_2 \times \mathbf{Z}_2$	$s_2, \gamma_{L/2}^y s_5, \gamma_{L/2}^x r$	$(x_1,0,x_3,-x_3)$	25
FROM LS=$(x,x,0,0)$					
$\lambda_2 = -2(A_7+A_8)x^2$	SQ	$\mathbf{D}_4$	s_1, s_4	(x_1,x_1,x_3,x_3)	12
$\lambda_2 = -2(A_7-A_8)x^2$	WS	$\mathbf{D}_4$	$\gamma_{L/2}^{xy} r s_1, s_6$	$(x_1,x_1,x_3,-x_3)$	24
$\lambda_2 + 2A_7 x^2 = 0$	$AR2$	$\mathbf{D}_2$	$s_4, \gamma_{L/2}^{xy} r s_2$	(x_1,x_2,ix_3,ix_3)	18
$\lambda_2 + 2A_7 x^2 = 0$	$WR2$	$\mathbf{D}_2$	$s_6, \gamma_{L/2}^{xy} r s_2$	$(x_1,x_1,ix_3,0)$	18
FROM SR=$(0,0,x,0)$					
$\lambda_1 + A_3 x^2 = 0$	$WR2$	$\mathbf{D}_2$	$\gamma_{L/2}^y r s_2, \gamma_{L/4}^{x,-y} s_6$	$(ix_1,x_1,x_3,0)$	26
$\lambda_1 + A_3 x^2 = 0$	$AR1$	$\mathbf{D}_2$	$s_2, \gamma_{L/2}^y r$	$(x_1,0,x_3,x_4)$	26
$\lambda_1 + A_3 x^2 = 0$	AS	$\mathbf{D}_2$	s_2, s_6	(x_1,x_1,x_3,x_4)	26
FROM SS=$(0,0,x,x)$					
$\lambda_1 + (2A_3+A_4)x^2 = 0$	SQ	$\mathbf{D}_4$	s_1, s_4	(x_1,x_1,x_3,x_3)	3
$\lambda_1 + (2A_3+A_4)x^2 = 0$	RC	$\mathbf{D}_2 \times \mathbf{Z}_2$	$s_2, s_5, \gamma_{L/2}^x r$	$(x_1,0,x_3,x_3)$	3
$\lambda_1 + (2A_3-A_4)x^2 = 0$	WS	$\mathbf{D}_4$	$\gamma_{L/2}^x r s_1, s_6$	(ix_1,ix_1,x_3,x_3)	32
$\lambda_1 + (2A_3-A_4)x^2 = 0$	$WR1$	$\mathbf{D}_2 \times \mathbf{Z}_2$	$s_4, \gamma_{L/2}^{xy} s_2, \gamma_{L/2}^x r$	$(ix_1,0,x_3,x_3)$	32

Table 3: *Branches of steady states bifurcating from LR, LS, SR and SS. Columns are the same as in Table 1.*

restricted to the respective subspace. The results of calculations are presented in the Table 4.

Bifurcations from secondary branches (see Table 5) are investigated the same way those from primary branches. Some of these bifurcations give rise to branches of drifting patterns (we refer to as travelling waves). Examples of such bifurcations are discussed in Appendix B.

3.4 Bifurcations from tertiary branches

Here we focus on bifurcations from AR1, AR2, AS and STW which all have symmetry groups isomorphic to $\mathbf{D}_2$. Methods and presentation are the same as above for more symmetric steady states. We do not list expressions for eigenvalues in the cases where isotypic components are 3-dimensional because they are unwieldy and uninformative. In Appendix C we give an example how bifurcations in a 3-d subspace can be studied without explicitly evaluating the eigenvalues. Tertiary branches and eigenvalues determining their stability are listed in Table 6, and possible bifurcations in Table 7.

3.5 Robust heteroclinic connections between steady states

A heteroclinic connection from one steady state to another one is robust only if there exists such a fixed point subspace for a subgroup of the system symmetry group such that the connection within that subspace is robust [14], for example if it is a saddle to sink connection. Examination of Table 2 reveals the possibility of robust heteroclinic connections given in Table 8 where we list pairs of steady states between which robust heteroclinic connections are possible.

The connections within subspaces listed in Table 8 can form homoclinic and heteroclinic cycles, e.g. the connection $SS \to SS$ implies existence of the respective homoclinic cycle. There are three subspaces in which connections between LS and SS are possible. If there exists a connection $LS \to SS$ in one of them, and $SS \to LS$ in another one, a heteroclinic cycle $LS \to SS \to LS$ emerges. The

Steady state	Typical point	Invariant subspaces	Eigenvalues	Action	Kernel
RC	$(x_1,0,x_3,x_3)$	$(q_1,0,q_3,q_3)$	$\mu_1+\mu_2 = 2A_1x_1^2 + 2(A_5+A_6)x_3^2$ $\mu_1\mu_2 = 4x_1^2x_3^2$ $\times(A_1(A_5+A_6)-(2A_3+A_4)(A_7+A_8))$	$\mathbf{1}$	all
		$(0,q,0,0)$	$(A_2-A_1)x_1^2$	$\mathbf{Z}_2$	s_2, s_5
		$(0,iq,0,0)$	$(A_2-A_1)x_1^2 - 2A_4x_3^2$	$\mathbf{Z}_2$	$s_5, \gamma^x_{L/2}rs_2$
		$(0,0,q,-q)$	$2(A_5-A_6)x_3^2 - 2A_8x_1^2$	$\mathbf{Z}_2$	$s_2, \gamma^x_{L/2}r$
		$(0,0,iq,-iq)$	0	$\mathbf{Z}_2$	$s_5, \gamma^x_{L/2}r$
		$(iq_1,0,iq_3,iq_3)$	$0, -2A_8x_1^2 - 2A_4x_3^2$	$\mathbf{Z}_2$	$s_4, \gamma^x_{L/2}r$
$WR1$	$(x_1,0,x_3,-x_3)$	$(q_1,0,q_3,-q_3)$	$\mu_1+\mu_2 = 2A_1x_1^2 + 2(A_5+A_6)x_3^2$ $\mu_1\mu_2 = 4x_1^2x_3^2$ $\times(A_1(A_5+A_6)-(2A_3-A_4)(A_7-A_8))$	$\mathbf{1}$	all
		$(0,q,0,0)$	$(A_2-A_1)x_1^2$	$\mathbf{Z}_2$	$s_2, \gamma^{xy}_{L/2}rs_5$
		$(0,iq,0,0)$	$(A_2-A_1)x_1^2 + 2A_4x_3^2$	$\mathbf{Z}_2$	$\gamma^x_{L/2}rs_2, \gamma^{xy}_{L/2}rs_5$
		$(0,0,q,q)$	$2(A_5-A_6)x_3^2 + 2A_8x_1^2$	$\mathbf{Z}_2$	$s_2, \gamma^x_{L/2}r$
		$(0,0,iq,iq)$	0	$\mathbf{Z}_2$	$\gamma^x_{L/2}r, \gamma^y_{L/2}s_5$
		$(iq_1,0,iq_3,-iq_3)$	$0, 2A_8x_1^2 + 2A_4x_3^2$	$\mathbf{Z}_2$	$\gamma^x_{L/2}r, \gamma^y_{L/2}s_4$
$WR2$	$(x_1,x_1,ix_3,0)$	$(q_1,q_1,iq_3,0)$	$\mu_1+\mu_2 = 2(A_1+A_2)x_1^2 + 2A_5x_3^2$ $\mu_1\mu_2 = 4x_1^2x_3^2((A_1+A_2)A_5 - 2A_3A_7)$	$\mathbf{1}$	all
		$(q_1,-q_1,0,iq_4)$	$\mu_1+\mu_2 = 2(A_1-A_2)x_1^2 + (A_6-A_5)x_3^2$ $\mu_1\mu_2 =$ $4x_1^2x_3^2((A_1-A_2)(A_6-A_5)-A_3A_8)$	$\mathbf{Z}_2$	$\gamma^{xy}_{L/2}rs_2$
		$(iq_1,-iq_1,0,0)$	0	$\mathbf{Z}_2$	$\gamma^{xy}_{L/2}rs_7$
		(iq_1,iq_1,q_3,q_4)	$\mu_1 = 0$ $\mu_2+\mu_3 = (A_6-A_5)x_3^2$ $\mu_2\mu_3 = -4A_8x_1^2(A_8x_1^2+A_4x_3^2)$	$\mathbf{Z}_2$	s_6
SQ	(x_1,x_1,x_3,x_3)	(q_1,q_1,q_3,q_3)	$\mu_1+\mu_2 = 2(A_1+A_2)x_1^2 + 2(A_5+A_6)x_3^2$ $\mu_1\mu_2 = 4x_1^2x_3^2$ $\times((A_1+A_2)(A_5+A_6)-2(2A_3+A_4)(A_7+A_8))$	$\mathbf{1}$	all
		$(q,-q,0,0)$	$2(A_1-A_2)x_1^2$	$\mathbf{Z}_2$	s_2, s_4
		$(0,0,q,-q)$	$2(A_5-A_6)x_3^2 - 4A_8x_1^2$	$\mathbf{Z}_2$	s_2, s_6
		(iq_1,iq_2,iq_3,iq_4)	$\mu_1=\mu_2=0$ $\mu_3=\mu_4 = -2A_8x_1^2 - 2A_4x_3^2$	$\mathbf{D}_4$	
WS	$(x_1,x_1,x_3,-x_3)$	$(q_1,q_1,q_3,-q_3)$	$\mu_1+\mu_2 = 2(A_1+A_2)x_1^2 + 2(A_5+A_6)x_3^2$ $\mu_1\mu_2 = 4x_1^2x_3^2$ $\times((A_1+A_2)(A_5+A_6)-2(2A_3-A_4)(A_7-A_8))$	$\mathbf{1}$	all
		$(q,-q,0,0)$	$2(A_1-A_2)x_1^2$	$\mathbf{Z}_2$	$s_2, \gamma^{xy}_{L/2}rs_5$
		$(0,0,q,q)$	$2(A_5-A_6)x_3^2 + 4A_8x_1^2$	$\mathbf{Z}_2$	s_2, s_6
		(iq_1,iq_2,iq_3,iq_4)	$\mu_1=\mu_2=0$ $\mu_3=\mu_4 = 2A_8x_1^2 + 2A_4x_3^2$	$\mathbf{D}_4$	

Table 4: *Invariant subspaces and associated eigenvalues determining stability of secondary steady states. Columns are the same as in Table 2.*

12

Bifurcates at	Name	Group	Generators	Typical point	No
FROM RC					
$2A_1x_1^2 + 2(A_5+A_6)x_3^2 = 0$	$P(RC)$	$\mathbf{D}_2 \times \mathbf{Z}_2$	$s_2, s_5, \gamma_{L/2}^x r$	$(x_1, 0, x_3, x_3)$ (periodic orbit)	
$(A_2-A_1)x_1^2 - 2A_4x_3^2 = 0$	$AR2$	$\mathbf{D}_2$	$s_5, \gamma_{L/2}^x r s_2$	(x_1, ix_2, x_3, x_3)	13
$(A_5-A_6)x_3^2 = A_8x_1^2$	$AR1$	$\mathbf{D}_2$	$s_2, \gamma_{L/2}^x r$	$(x_1, 0, x_3, x_4)$	5
$A_8x_1^2 = -A_4x_3^2$	STW	$\mathbf{D}_2$	$s_4, \gamma_{L/2}^x r$	$(z_1, 0, z_3, z_3) =$ $(r_1, 0, r_3, r_3, \phi, 0)$	8
FROM WR1					
$2A_1x_1^2 + 2(A_5+A_6)x_3^2 = 0$	$P(WR1)$	$\mathbf{D}_2 \times \mathbf{Z}_2$	$s_2, \gamma_{L/2}^y s_5, \gamma_{L/2}^x r$	$(x_1, 0, x_3, -x_3)$ (periodic orbit)	
$(A_2-A_1)x_1^2 + 2A_4x_3^2 = 0$	$AR2$	$\mathbf{D}_2$	$\gamma_{L/2}^y s_4, \gamma_{L/2}^x r s_2$	$(x_1, ix_2, x_3, -x_3)$	
$(A_5-A_6)x_3^2 + A_8x_1^2 = 0$	$AR1$	$\mathbf{D}_2$	$s_2, \gamma_{L/2}^x r$	$(x_1, 0, x_3, x_4)$	
$A_8x_1^2 + A_4x_3^2 = 0$	STW	$\mathbf{D}_2$	$\gamma_{L/2}^y s_4, \gamma_{L/2}^x r$	$(z_1, 0, z_3, -z_3) =$ $(r_1, 0, r_3, r_3, \phi, \pi)$	31
FROM WR2					
$(A_1+A_2)x_1^2 + 2A_5x_3^2 = 0$	$P(WR2)$	$\mathbf{D}_2$	$s_6, \gamma_{L/2}^{xy} r s_2$	$(x_1, x_1, ix_3, 0)$ (periodic orbit)	
$(A_1-A_2)(A_6-A_5) - A_3A_8 = 0$	NS	$\mathbf{Z}_2$	$\gamma_{L/2}^{xy} r s_2$	(x_1, x_2, ix_3, ix_4)	
$2(A_1-A_2)x_1^2 + (A_6-A_5)x_3^2 = 0$	$P(NS)$	$\mathbf{Z}_2$	$\gamma_{L/2}^{xy} r s_2$	(x_1, x_2, ix_3, ix_4) (periodic orbit)	20
$A_8x_1^2 + A_4x_3^2 = 0$	$TW4$	$\mathbf{Z}_2$	s_6	$(z_1, z_1, z_3, z_4) =$ $(r_1, r_1, r_3, r_4, \phi, -\phi)$	19
FROM SQ					
$(A_1+A_2)x_1^2 + (A_5+A_6)x_3^2 = 0$	$P(SQ)$	$\mathbf{D}_4$	s_1, s_4	(x_1, x_1, x_3, x_3) (periodic orbit)	
$(A_5-A_6)x_3^2 - 2A_8x_1^2 = 0$	AS	$\mathbf{D}_2$	s_2, s_6	(x_1, x_1, x_3, x_4)	4
$A_8x_1^2 + A_4x_3^2 = 0$	$TW2$	$\mathbf{Z}_2$	s_4	$(z_1, x_2, z_3, z_3) =$ $(r_1, r_2, r_3, r_3, \phi, 0)$	9
$A_8x_1^2 + A_4x_3^2 = 0$	$TW4$	$\mathbf{Z}_2$	s_6	$(z_1, z_1, z_3, z_4) =$ $(r_1, r_1, r_3, r_4, \phi, \phi)$	9
FROM WS					
$(A_1+A_2)x_1^2 + (A_5+A_6)x_3^2 = 0$	$P(WS)$	$\mathbf{D}_4$	$\gamma_{L/2}^{xy} r s_1, s_6$	$(x_1, x_1, x_3, -x_3)$ (periodic orbit)	
$(A_5-A_6)x_3^2 + 2A_8x_1^2 = 0$	AS	$\mathbf{D}_2$	s_2, s_6	(x_1, x_1, x_3, x_4)	
$A_8x_1^2 + A_4x_3^2 = 0$	$TW3$	$\mathbf{Z}_2$	$\gamma_{L/2}^{xy} r s_4$	$(z_1, x_2, z_3, -z_3) =$ $(r_1, r_2, r_3, r_3, \phi, \pi)$	27
$A_8x_1^2 + A_4x_3^2 = 0$	$TW4$	$\mathbf{Z}_2$	s_6	$(z_1, z_1, z_3, z_4) =$ $(r_1, r_1, r_3, r_4, \phi, -\phi)$	27

Table 5: *Bifurcations from secondary steady states. Columns are the same as in Table 1. $P(M)$ indicates there is bifurcation to periodic orbits with instantaneous symmetry equal to that of M.*

Steady state	Typical point	Invariant subspaces	Eigenvalues	Action	Kernel
$AR1$	$(x_1, 0, x_3, x_4)$	$(q_1, 0, q_3, q_4)$	μ_1, μ_2, μ_3	**1**	all
		$(iq_1, 0, iq_3, iq_4)$	$0, 0, -A_8 x_1^2 (x_4/x_3 + x_3/x_4) - 2A_4 x_3 x_4$	$\mathbf{Z}_2$	$\gamma_{L/2}^x r$
		$(0, q, 0, 0)$	$(A_2 - A_1) x_1^2$	$\mathbf{Z}_2$	s_2
		$(0, iq, 0, 0)$	$(A_2 - A_1) x_1^2 - 2A_4 x_3 x_4$	$\mathbf{Z}_2$	$\gamma_{L/2}^x r s_2$
$AR2$	(x_1, ix_2, x_3, x_3)	(q_1, iq_2, q_3, q_3)	μ_1, μ_2, μ_3	**1**	all
		$(iq_1, 0, iq_3, iq_3)$	$0, -2A_8 x_1^2 - 2A_4 x_3^2$	$\mathbf{Z}_2$	$\gamma_{L/2}^x s_4$
		$(0, q_2, iq_3, -iq_3)$	$0, 2A_8 x_2^2 + 2A_4 x_3^2$	$\mathbf{Z}_2$	s_5
		$(0, 0, q, -q)$	$2A_8(-x_1^2 + x_2^2) + 2(A_5 - A_6) x_3^2$	$\mathbf{Z}_2$	$\gamma_{L/2}^x s_2$
AS	(x_1, x_1, x_3, x_4)	(q_1, q_1, q_3, q_4)	μ_1, μ_2, μ_3	**1**	all
		$(iq_1, iq_1, iq_3, 0)$	$0, -2A_8 x_1^2 x_4/x_3 - 2A_4 x_3 x_4$	$\mathbf{Z}_2$	s_6
		$(iq_1, -iq_1, 0, iq_4)$	$0, -2A_8 x_1^2 x_3/x_4 - 2A_4 x_3 x_4$	$\mathbf{Z}_2$	s_7
		$(q, -q, 0, 0)$	$2(A_1 - A_2) x_1^2$	$\mathbf{Z}_2$	s_2
STW	$(z_1, 0, z_3, z_3) =$	$(q_1, 0, q_2, q_2, \xi, 0)$	μ_1, μ_2, μ_3	**1**	all
	$(r_1, 0, r_3, r_3, \phi, 0)$	$(0, q, 0, 0)$	$(A_2 - A_1) r_1^2 + A_4 r_3^2 (1 - \cos\phi)$	$\mathbf{Z}_2$	s_4
		$(0, iq, 0, 0)$	$(A_2 - A_1) r_1^2 - A_4 r_3^2 (1 + \cos\phi)$	$\mathbf{Z}_2$	$\gamma_{L/2}^x r s_4$
		$(0, 0, w, -w)$	$0, 2(A_5 - A_6) r_3^2 - 2A_8 r_1^2 \cos\phi$	$\mathbf{Z}_2$	$\gamma_{L/2}^x r$

Table 6: *Invariant subspaces and associated eigenvalues determining stability of tertiary branches of relative equilibria. Note that AR1, AR2, AS are steady solutions whereas STW are drifting (travelling waves). Columns are the same as in Table 2.*

system can possess other types of heteroclinic cycles, for example $LR \to SS \to LR$ and $LS \to SS \to SR \to LS$, and much more intricate heteroclinic networks.

The two-dimensional subspaces listed in Table 8 are of special interest because for them it is possible to derive analytically a sufficient condition for existence of a heteroclinic connection. Existence of the connection if one state of a pair is stable and another one is unstable is implied by the following Theorem that is a modification of Theorem 1 in [10].

Theorem 1 *Consider the system*

$$\dot{x} = \lambda x + B_1 x^3 + B_2 x y^2,$$

$$\dot{y} = \mu y + C_1 y^3 + C_2 x^2 y.$$

If $\lambda > 0$, $\mu > 0$, $B_1 < 0$, $C_1 < 0$, $\lambda - B_2\mu/C_1 > 0$, $\mu - C_2\lambda/B_1 < 0$, then the only steady states of the system are $(0,0)$, $S_1 = \left(\pm\sqrt{-\lambda/B_1}, 0\right)$, $S_2 = \left(0, \pm\sqrt{-\mu/C_1}\right)$ and there exists a robust heteroclinic connection from S_1 to S_2.

4 Analysis of bifurcations of the reduced system

Consider the original motivating hydrodynamic problem of Boussinesq convection in a layer Eq. (1)-Eq. (4) for parameters k and R close to the mode interaction point (k_m, R_m) shown in Figure 1. We set

$$\epsilon = R - R_m, \quad \delta = k - k_m, \tag{14}$$

and assume ϵ and δ are small, so that a centre manifold approximation performed in the vicinity of (k_m, R_m) is valid. Details of calculation of the normal form Eq. (12) coefficients are given in

Bifurcates at	Name	Group	Generators	Typical point	No
FROM AR1					
$\mu_1 = i\omega, \mu_2 = -i\omega$	$P(AR1)$	$\mathbf{D}_2$	$s_2, \gamma^x_{L/2}r$	$(x_1,0,x_3,x_4)$ (periodic orbit)	7
$A_8 x_1^2 (x_4/x_3 + x_3/x_4) + A_4 x_3 x_4 = 0$	$TW1$	$\mathbf{Z}_2$	$\gamma^x_{L/2}r$	$(z_1,0,z_3,z_4) = (r_1,0,r_3,r_4,\phi,\psi)$	11
$(A_2 - A_1)x_1^2 - 2A_4 x_3 x_4 = 0$	NS	$\mathbf{Z}_2$	$\gamma^x_{L/2}r s_2$	(x_1,ix_2,x_3,x_4)	
FROM AR2					
$\mu_1 = i\omega, \mu_2 = -i\omega$	$P(AR2)$	$\mathbf{D}_2$	$s_5, \gamma^y_{L/2}r s_2$	(x_1,ix_2,x_3,x_3) (periodic orbit)	
$A_8 x_1^2 + A_4 x_3^2 = 0$	$TW3$	$\mathbf{Z}_2$	$\gamma^x_{L/2}r s_4$	$(z_1,ix_2,z_3,z_3) = (r_1,r_2,r_3,r_3,\phi,\pi)$	
$A_8 x_2^2 + A_4 x_3^2 = 0$	$TW2$	$\mathbf{Z}_2$	s_5	$(x_1,z_2,z_3,\bar{z}_3) = (r_1,r_2,r_3,r_3,0,\phi)$	14
$A_8(-x_1^2 + x_2^2) + (A_5 - A_6)x_3^2 = 0$	NS	$\mathbf{Z}_2$	$\gamma^y_{L/2}r s_2$	(x_1,ix_2,x_3,x_4)	
FROM AS					
$\mu_1 = i\omega, \mu_2 = -i\omega$	$P(AS)$	$\mathbf{D}_2$	s_2, s_6	(x_1,x_1,x_3,x_4) (periodic orbit)	6
$A_8 x_1^2 x_4/x_3 + A_4 x_3 x_4 = 0$	$TW4$	$\mathbf{Z}_2$	s_6	$(z_1,z_1,z_3,x_4) = (r_1,r_1,r_3,r_4,\phi,\phi)$	
$A_8 x_1^2 x_3/x_4 + A_4 x_3 x_4 = 0$	$TW4$	$\mathbf{Z}_2$	s_7	$(z_1,\bar{z}_1,x_3,z_4) = (r_1,r_1,r_3,r_4,\phi,-\phi)$	10
FROM STW					
$\mu_1 = i\omega, \mu_2 = -i\omega$	$P(STW)$	$\mathbf{D}_2$	$s_4, \gamma^x_{L/2}r$	$(z_1,0,z_3,z_3)$ (periodic orbit)	28
$(A_2 - A_1)r_1^2 + A_4 r_3^2(1-\cos\phi) = 0$	$TW2$	$\mathbf{Z}_2$	s_4	$(z_1,x_2,z_3,z_3) = (r_1,r_2,r_3,r_3,\phi,0)$	
$(A_2 - A_1)r_1^2 - A_4 r_3^2(1+\cos\phi) = 0$	$TW3$	$\mathbf{Z}_2$	$\gamma^x_{L/2}r s_4$	$(z_1,ix_2,z_3,z_3) = (r_1,r_2,r_3,r_3,\phi,\pi)$	30
$2(A_5 - A_6)r_3^2 - 2A_8 r_1^2 \cos\phi = 0$	$TW1$	$\mathbf{Z}_2$	$\gamma^x_{L/2}r$	$(z_1,0,z_3,z_4) = (r_1,0,r_3,r_4,\phi,\psi)$	21

Table 7: *Bifurcations from tertiary branches. Columns are the same as in Table 1.*

Subspace	Subgroup	Generators	Steady states	Eigenspaces	Eigenvalues
(q_1, q_2, iq_3, iq_3)	$\mathbf{D}_2$	$s_4, \gamma_{L/2}^{xy} r s_2$	$LR = (x,0,0,0)$	$(q,0,0,0)$	$-2\lambda_1$
				$(0,q,0,0)$	$\lambda_1(A_1 - A_2)/A_1$
				$(0,0,iq,iq)$	$\lambda_2 + (A_7 - A_8)x_1^2$
			$LR = (0,x,0,0)$	$(0,q,0,0)$	$-2\lambda_1$
				$(q,0,0,0)$	$\lambda_1(A_1 - A_2)/A_1$
				$(0,0,iq,iq)$	$\lambda_2 + (A_7 + A_8)x_1^2$
$(q_1, q_2, 0, 0)$	$\mathbf{D}_2 \times \mathbf{Z}_2$	$s_2, s_4, \gamma_{L/2}^{xy} r$	$LR = (x_1,0,0,0)$	$(q,0,0,0)$	$-2\lambda_1$
				$(0,q,0,0)$	$\lambda_1(A_1 - A_2)/A_1$
			$LS = (x_2,x_2,0,0)$	$(q,q,0,0)$	$-2\lambda_1$
				$(q,-q,0,0)$	$\lambda_1(A_2 - A_1)/(A_1 + A_2)$
$(0, 0, q_1, q_2)$	$\mathbf{D}_2 \times \mathbf{Z}_2$	$s_2, s_6, \gamma_{L/2}^{xy}$	$SR = (0,0,x_1,0)$	$(0,0,q,0)$	$-2\lambda_2$
				$(0,0,0,q)$	$\lambda_2(A_5 - A_6)/A_5$
			$SS = (0,0,x_2,x_2)$	$(0,0,q,q)$	$-2\lambda_2$
				$(0,0,q,-q)$	$\lambda_2(A_6 - A_5)/(A_6 + A_5)$
$(q_1, 0, q_2, q_3)$	$\mathbf{D}_2$	$s_2, \gamma_{L/2}^{x} r$	$SS = (0,0,x,x)$	$(0,0,q,q)$	$-2\lambda_2$
				$(0,0,q,-q)$	$\lambda_2(A_6 - A_5)/(A_6 + A_5)$
				$(q,0,0,0)$	$\lambda_1 + (2A_3 + A_4)x^2$
			$SS = (0,0,-x,x)$	$(0,0,-q,q)$	$-2\lambda_2$
				$(0,0,q,q)$	$\lambda_2(A_6 - A_5)/(A_6 + A_5)$
				$(q,0,0,0)$	$\lambda_1 + (2A_3 - A_4)x^2$
$(q_1, 0, q_2, q_3)$	$\mathbf{D}_2$	$s_2, \gamma_{L/2}^{x} r$	$LR = (x_1,0,0,0)$	$(q,0,0,0)$	$-2\lambda_1$
				$(0,0,q,q)$	$\lambda_2 + (A_7 + A_8)x_1^2$
				$(0,0,q,-q)$	$\lambda_2 + (A_7 - A_8)x_1^2$
			$SR = (0,0,x_2,0)$	$(0,0,q,0)$	$-2\lambda_2$
				$(0,0,0,q)$	$\lambda_2(A_5 - A_6)/A_5$
				$(q,0,0,0)$	$\lambda_1 + A_3 x_2^2$
$(q_1, 0, q_2, q_2)$	$\mathbf{D}_2 \times \mathbf{Z}_2$	$s_2, s_4, \gamma_{L/2}^{x} r$	$LR = (x_1,0,0,0)$	$(q,0,0,0)$	$-2\lambda_1$
				$(0,0,q,q)$	$\lambda_2 + (A_7 + A_8)x_1^2$
			$SS = (0,0,x_2,x_2)$	$(0,0,q,q)$	$-2\lambda_2$
				$(q,0,0,0)$	$\lambda_1 + (2A_3 + A_4)x_2^2$
$(q_1, 0, q_2, -q_2)$	$\mathbf{D}_2 \times \mathbf{Z}_2$	$s_2, \gamma_{L/2}^{y} s_4, \gamma_{L/2}^{x} r$	$LR = (x_1,0,0,0)$	$(q,0,0,0)$	$-2\lambda_1$
				$(0,0,q,-q)$	$\lambda_2 + (A_7 - A_8)x_1^2$
			$SS = (0,0,x_2,-x_2)$	$(0,0,q,-q)$	$-2\lambda_2$
				$(q,0,0,0)$	$\lambda_1 + (2A_3 - A_4)x_2^2$

Table 8: *Fixed points subspaces for subgroups of $\mathbf{D}_4 \ltimes \mathbf{T}^2 \times \mathbf{Z}_2$, in which robust heteroclinic connections are possible. Shown are: a typical point of a subspace (where q_k are real quantities), symmetry group, its generators, the steady states, eigenspaces, and associated eigenvalues.*

Subspace	Subgroup	Generators	Steady states	Eigenspaces	Eigenvalues
(q_1,q_1,q_2,q_2)	$\mathbf{D}_4$	s_1,s_4	$LS=(x_1,x_1,0,0)$	$(q,q,0,0)$	$-2\lambda_1$
				$(0,0,q,q)$	$\lambda_2+2(A_7+A_8)x_1^2$
			$SS=(0,0,x_2,x_2)$	$(0,0,q,q)$	$-2\lambda_2$
				$(q,q,0,0)$	$\lambda_1+(2A_3+A_4)x_2^2$
$(q_1,q_1,q_2,-q_2)$	$\mathbf{D}_4$	$\gamma_{L/2}^{xy}rs_1,s_6$	$LS=(x_1,x_1,0,0)$	$(q,q,0,0)$	$-2\lambda_1$
				$(0,0,q,-q)$	$\lambda_2+2(A_7-A_8)x_1^2$
			$SS=(0,0,x_2,-x_2)$	$(0,0,q,-q)$	$-2\lambda_2$
				$(q,q,0,0)$	$\lambda_1+(2A_3-A_4)x_2^2$
(q_1,q_2,iq_3,iq_3)	$\mathbf{D}_2$	$s_4,\gamma_{L/2}^{xy}rs_2$	$LS=(x_1,x_1,0,0)$	$(q,q,0,0)$	$-2\lambda_1$
				$(q,-q,0,0)$	$\lambda_1(A_2-A_1)/(A_2+A_1)$
				$(0,0,iq,iq)$	$\lambda_2+2A_7x_1^2$
			$SS=(0,0,ix_2,ix_2)$	$(0,0,iq,iq)$	$-2\lambda_2$
				$(q,0,0,0)$	$\lambda_1+(2A_3-A_4)x_2^2$
				$(0,q,0,0)$	$\lambda_1+(2A_3+A_4)x_2^2$
$(q_1,q_1,iq_2,0)$	$\mathbf{D}_2$	$s_6,\gamma_{L/2}^{xy}rs_2$	$LS=(x_1,x_1,0,0)$	$(q,q,0,0)$	$-2\lambda_1$
				$(0,0,iq,0)$	$\lambda_2+2A_7x_1^2$
			$SR=(0,0,ix_2,0)$	$(0,0,iq,0)$	$-2\lambda_2$
				$(q,q,0,0)$	$\lambda_1+A_3x_2^2$
(q_1,q_1,q_3,q_4)	$\mathbf{D}_2$	s_2,s_6	$LS=(x_1,x_1,0,0)$	$(q,q,0,0)$	$-2\lambda_1$
				$(0,0,q,q)$	$\lambda_2+(A_7+A_8)x_1^2$
				$(0,0,q,-q)$	$\lambda_2+(A_7-A_8)x_1^2$
			$SR=(0,0,x_2,0)$	$(0,0,q,0)$	$-2\lambda_2$
				$(0,0,0,q)$	$\lambda_2(A_5-A_6)/A_5$
				$(q,q,0,0)$	$\lambda_1+A_3x_2^2$

Continuation of Table 8.

β_{ij}	$j = 1$	$j = 2$
$i = 1$	3.1551	0.01949
$i = 2$	-4.2921	0.02456

α_{ij}	$j = 1$	$j = 2$	$j = 3$
$i = 1$	0	0	-0.125
$i = 2$	-0.03207	-0.01843	-0.18081
$i = 3$	0.02281	0.13589	-0.1744
$i = 4$	-0.08110	-0.3240	-0.1441
$i = 5$	0	0	-0.125
$i = 6$	-0.03108	-0.01958	-0.17434
$i = 7$	-0.1954	-0.2513	-0.2667
$i = 8$	0.1314	0.2237	-0.1096

Table 9: *The coefficients α_{ij} and β_{ij} in Eq. (15, 16) that determine the coefficients A_i and λ_i of the normal form Eq. (12).*

Appendices D, E and F. The coefficients have dependence on P given by

$$\lambda_i = P(P+1)^{-1}(\beta_{i1}\delta + \beta_{i2}\epsilon) + O(\epsilon^2 + \delta^2) \tag{15}$$

$$A_i = P(P+1)^{-1}(P^{-2}\alpha_{i1} + P^{-1}\alpha_{i2} + \alpha_{i3}) + O(|\epsilon| + |\delta|). \tag{16}$$

The values of α_{ij} and β_{ij} are listed in Table 9. The α's agree with those in [20]: if the variables in Eq. (12) are rescaled $z_i \to \gamma_i z_i$ with $\gamma_1 = \gamma_2 = \sqrt{A_1^{RM}/A_1}$ and $\gamma_3 = \gamma_4 = \sqrt{A_5^{RM}/A_5}$, where the superscript PM denotes the respective coefficients in the paper [20], the values of α's differ only in the last shown digit.

4.1 A summary of bifurcations for the reduced system for fixed P

We investigate the dynamics of the Boussinesq problem near (k_m, R_m) shown on Figure 1 for a range of Prandtl numbers P. We use numerical path following [8] and the results from Section 3.

We produce gyrant bifurcation diagrams that show the bifurcating branches on varying parameters around a small circle in the (k, R) plane that encloses the mode interaction. These are found by taking parameters θ and r that determine the growth rates of the primary modes

$$\lambda_1 = r\cos\theta, \quad \lambda_2 = r\sin\theta \tag{17}$$

and investigating the behavior of Eq. (12) with coefficients as in Eq. (15,16) determined by centre manifold reduction. The cubic truncation the dynamics does not qualitatively depend on r as r can be scaled to be unity by a change in timescale.

Figure 4 gives some bifurcation diagrams calculated in this way for a range of Prandtl numbers, where the locations of the labelled bifurcations are listed in Table 10 and θ increases from $-\pi/2$ at *1* to π at *33*. Solid single lines correspond to relative equilibria that are stable if the lines are bold. Dashed lines correspond to periodic solutions that are similarly stable if the lines are bold. Wavy line denotes chaotic attractors. Double lines indicate that there are robust heteroclinic networks that exist in this region; these correspond to attractors if the lines are bold. The double lines start and end at steady bifurcations where robust cycles are created. However they do not indicate all the steady branches and bifurcations involved in the network.
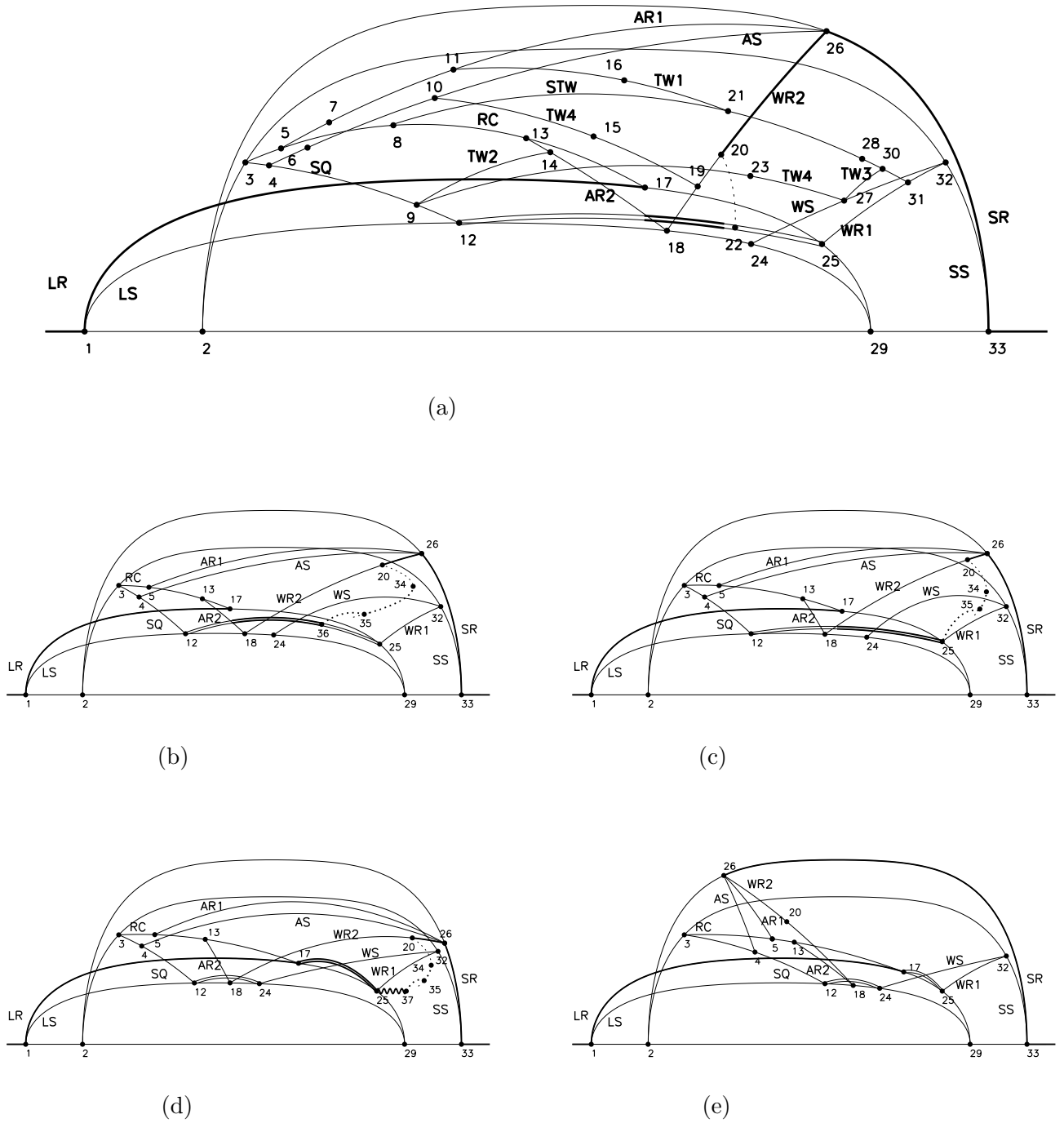
18

Figure 4: *Bifurcation diagrams for the reduced normal form equations for a range of Prandtl numbers; (a) P = 1, (b) P = 0.5, (c) P = 0.3, (d) P = 0.1, (e) P = 2. The horizontal axis (not shown to uniform scale) shows θ varying from −π/2 (labelled 1) to π (labelled 34). Only one representative of each branch is illustrated, and the vertical axis represents a solution norm that is also not to scale. All primary and secondary branches along with selected tertiary branches are shown. The only periodic branches shown are those bifurcating from stable states.*

19

P = 1

	1	2	3	4	5	6	7	8	9	10	11	12
θ	−π/2	0	0.5425	0.6609	0.7078	0.8524	0.8845	1.019	1.057	1.127	1.136	1.2067
	13	14	15	16	17	18	19	20	21	22	23	24
θ	1.2240	1.262	1.264	1.279	1.3095	1.3259	1.330	1.3444	1.352	1.353	1.372	1.3870
	25	26	27	28	29	30	31	32	33			
θ	1.4411	1.4458	1.511	1.522	π/2	1.571	1.666	2.547	π			

P = 0.5

	1	2	3	4	5	12	13	17	18	24
θ	−π/2	0	0.559	0.670	0.687	1.240	1.306	1.390	1.420	1.473
	36	35	25	20	29	34	26	32	33	
θ	1.500	1.508	1.519	1.547	π/2	1.646	2.557	2.842	π	

P = 0.3

	1	2	3	4	5	12	13	18	17	24
θ	−π/2	0	0.590	0.703	0.727	1.272	1.379	1.460	1.465	1.503
	25	29	35	20	34	26	32	33		
θ	1.548	π/2	1.602	1.625	1.76	2.911	2.923	π		

P = 0.1

	1	2	3	4	5	12	13	18	24	17
θ	−π/2	0	0.668	0.803	0.842	1.313	1.464	1.484	1.522	1.553
	25	29	37	20	35	34	32	26	33	
θ	1.567	π/2	1.645	1.647	1.660	1.85	2.948	3.106	π	

P = 2

	1	2	3	26	4	5	20	13	12	18	24	17
θ	−π/2	0	0.54	0.89	0.92	0.96	1.13	1.18	1.20	1.23	1.24	1.28
	25	29	32	33								
θ	1.32	π/2	1.95	π								

Table 10: *This table gives the locations of the bifurcations shown in Figure 4 on increasing θ from left to right for a small circuit around the mode interaction at (k_m, R_m). The labels are sequential for $P = 1$ but change ordering for different values of P.*

For $P = 1$ we observe the following sequence of attractors on increasing θ. Referring to the numbered bifurcations in Figure 4(a) up to point *1* the trivial solution is stable. At *1* (corresponding to $\lambda_1 = 0$ and $\lambda_2 < 0$) there is bifurcation to stable LR. These persist up to *17* where there is a bifurcation to RC with no nearby stable states. In the interval *17-20* the only attractor is a robust heteroclinic attractor that we describe in detail in Section 4.3. At *20* there is a subcritical Hopf bifurcation that stabilizes WR2 and that apparently destroys the stable heteroclinic attractor. The branch of WR2 is stable to *26* where it branches from and stabilizes the SR state. The latter finally disappears at point *33* (corresponding to $\lambda_2 = 0$ and $\lambda_1 < 0$).

For $P = 0.5$ Figure 4(b) shows a similar sequence of bifurcations as for $P = 1$ except that the ordering and criticality of some of the steady bifurcations has changed. In addition there is a limit point *34* on the branch of subcritically branching periodic solutions from WR2 at *20*. This gives rise to bistability of the WR2 solution with large amplitude periodic orbits in the interval from *20* to *34*. These large amplitude periodic orbits form the only attractors for *20* to *35*. As we move from *35* down to *36* there is a complicated sequence of bifurcations of periodic orbits and chaotic attractors that may be evidence of structural instability in this region. At the end of this sequence of bifurcations there is an attracting heteroclinic network between *17* and *36*.

For $P = 0.3$ and 0.1 (Figures4(c) and (d) respectively) the heteroclinic network is attracting up to *25* where the last cyclic connections are destroyed by bifurcation from LR to WR1. In both cases there is bistability of periodic solutions and WR2 in the region from *35* to *34* and a complicated sequence of bifurcations including period doubling and symmetry breaking of periodic orbits between *25* and *34*. The main difference between the cases $P = 0.3$ and $P = 0.1$ is that the bifurcations *17* and *24* change order meaning that the region of existence of robust heteroclinic cycles splits into two intervals for $P = 0.1$. After destruction of the heteroclinic cycle at *25* there are highly intermittent chaotic attractors between *25* and *37*. An example of such an attractor is shown in Figure 5 for $P = 0.1$ and $\theta = 1.58$.

Finally for $P = 2$ Figure 4(e) shows the dynamical complexity is reduced for the attractors; there is simply bistability of LR and SR of the whole region from *26* to *17* and apparently no other attractors. There are still robust heteroclinic cycles from *12* to *24* and from *17* to *25* but they are not attracting.

4.2   Bifurcations for the reduced system on varying P

The main (primary and secondary) bifurcations of the normal form Eq. (12) with coefficients Eq. (15,16) and (17) are shown on Figure 6. This illustrates the variation of the bifurcation points in Figure 4 with P. Tertiary and Hopf bifurcations are not shown in this diagram.

To the left of the line *17* there are stable LR solutions while to the right of *26* up the line *33* there are stable SR solutions. The attracting heteroclinic cycles exist within the region enclosed by *17*, *26* and $P = 0$. Tables 1 and 3 imply that lines *17* and *26* intersect at P_c such that

$$A_3(A_7 + A_8) = A_1 A_5.$$

Substituting in Eq. (16) with coefficient values listed in Table 9 and solving the equation for P numerically we obtain $P_c \approx 1.118$. For $P > P_c$ there is an interval of θ where stable LR and SR coexist; for any θ at least one stable steady state is always present. This implies that the heteroclinic network of the type considered in subsection 4.3 (or its subcycle) can not be an attractor or a part of an attractor for $P > P_c$. To see this, suppose that a heteroclinic attractor of the type considered in 4.3 exists in the system. For $P > P_c$ at least one of SR or LR is stable. Let it be SR. Hence, SR does not belong to the heteroclinic attractor. Hence, SS belongs to the attractor. (Any subcycle involves either SR or SS.) A connection from SS to SR exists for all P, and a trajectory close to the assumed attractor finally will be attracted by the stable SR.
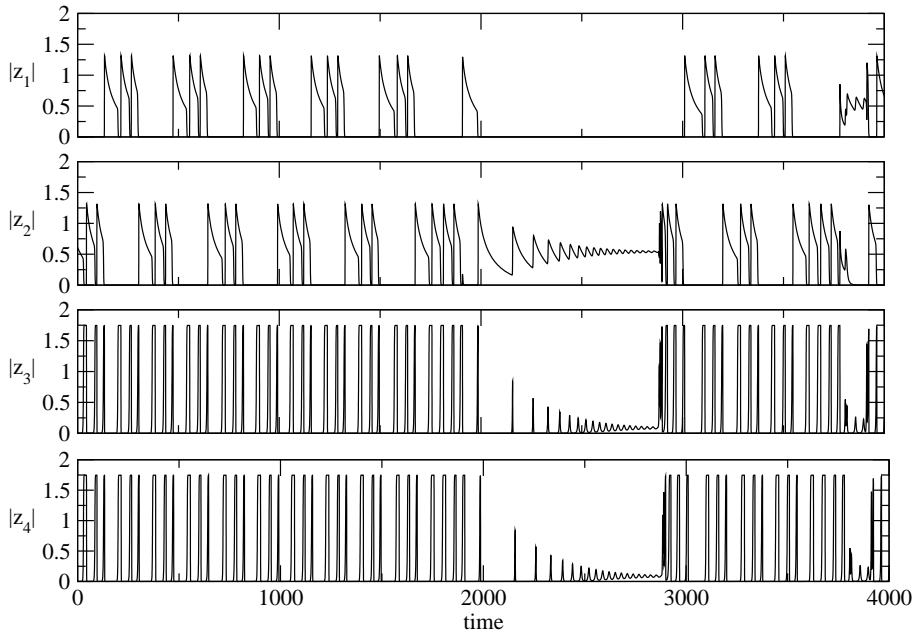
Figure 5: *Example of a chaotic attractor in the system for $P = 0.1$ and $\theta = 1.58$. For $t < 2000$ the trajectory appears to be on a periodic orbit that is close to a heteroclinic cycle, while for $2000 < t < 3000$ there is a transition to WR2 after which (for $2900 < t < 3000$) it returns to the orbit. For $k = 1.84$, employed in numerical investigation of convective attractors, the Rayleigh number corresponding to $\theta = 1.58$ is $R = 687.0$.*

The directions of branching and stability of bifurcating solutions in bifurcation of SR are different for different P. Appendix A demonstrates that that bifurcation from SR gives three bifurcating branches. Only one of branches can be stable, and that only if all three bifurcate supercritically, the two remaining branches being unstable. Moreover the stable one has the largest amplitude. The steady state WR2 bifurcates supercritically for $P < P_r$, where P_r is the value for which the lines marked *26* and *18* on Figure 6 intersect. P_r is a root of the equation

$$2A_3A_7 = A_5(A_1 + A_2).$$

Substituting here Eq. (16) with the coefficient values listed in Table 9 and solving the resultant equation numerically we obtain $P_r \approx 1.110$. We have checked that for $P < P_r$ the steady state WR2 has the largest amplitude (amplitudes were calculated from Tables 3 and 9) and two other steady states bifurcate supercritically. Therefore, for $P < P_r$ stable WR2 bifurcate from SR, and for $P > P_r$ no stable branches bifurcate from it.

We remark that there are codimension two bifurcation points at all crossings of lines in the (θ, P) plane. These are typically degenerate for the cubic truncation of the normal form; for example there is a vertical branch of WR2 on crossing of the lines *18* and *26* that can only be resolved by including fifth order terms in Eq. (12).

4.3 Heteroclinic attractors for $P = 1$

We study the heteroclinic attractors in the case $P = 1$ in more detail, for parameters in the interval between *17* and *20* in Figure 4(a).
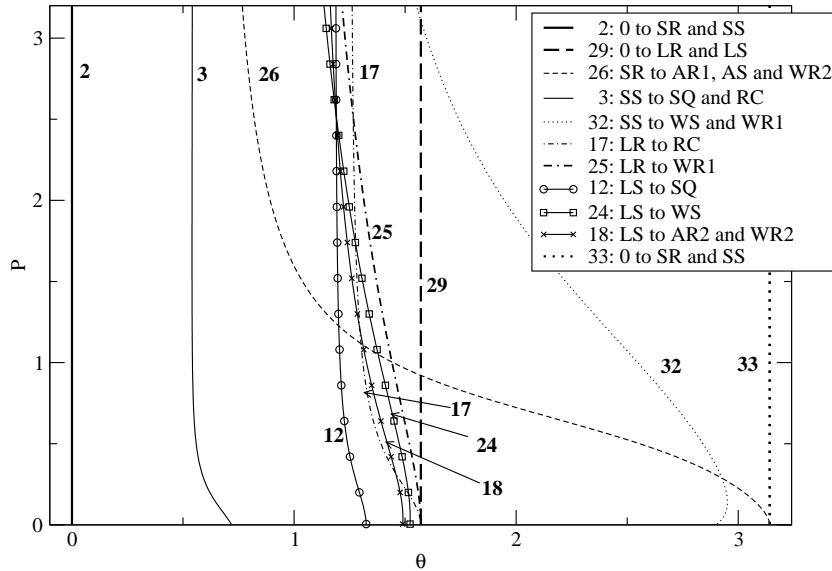
22

Figure 6: *Two parameter bifurcation diagram showing the location of the primary and secondary bifurcations for a range of θ and P. The numbering is the same as on Figure 4. Note that the bifurcation number 1 is not shown because it is to the left of this diagram at $\theta = -\pi/2$.*

For the sub-interval between *19* and *20* the attractor is not a conventional type of heteroclinic cycle but also includes connections from within the cycle to a subcycle; this means that the network has depth two in the terminology of [1]. As such this the first example of a depth two cycle in a fluid dynamical system.

Figure 7 schematically illustrates the structures of attractor for parameters in this range as far as we have been able to determine. On increasing θ the first bifurcation at *17* creates the LR→SS→LR cycle at disappearance of the branch of RC. The full dynamics of all connections in the interval between *17* and *18* is not clear but there are robust connections from AS and AR1 to the cycle between LR and SS. Between *18* and *20* there is a connection from WR2 to the cycle that affects the dynamics also for nearby θ as shown in Figure 8. This Figure shows the evolution of amplitudes of modes $|z_i|$ for a randomly chosen initial condition for $P = 1$ and $\theta = 1.325$. After an initial slowing down oscillation between LR and SS states the trajectory takes an alternative route on the unstable manifold at approximately $t = 1000$ that takes it close to SR, then AR1 and at approximately $t = 3300$ towards a state near where WR2 is created. The process then repeats by approaching the LR-SS cycle.

5 Numerical simulations of convective attractors

In this section we present results of numerical investigation of attractors of Boussinesq convection Eq. (1)-Eq. (4). Computations have been performed using the standard pseudospectral methods and a 4th order Runge-Kutta scheme for integration in time (see details in [17]) for $P = 0.1$, 0.3, 0.5, 1 and 2, $\delta = \pm 0.01 k_m$ (i. e. $k = 1.84$ and 1.88) and R increasing from 0. A small value of δ has been chosen so that the third-order truncated normal form can be expected to be valid.

Attractors found in numerical simulations are listed in Table 11, where intervals of existence of attractors are given in terms of both R and θ, where θ is calculated from R using Eq. (14), (15) and
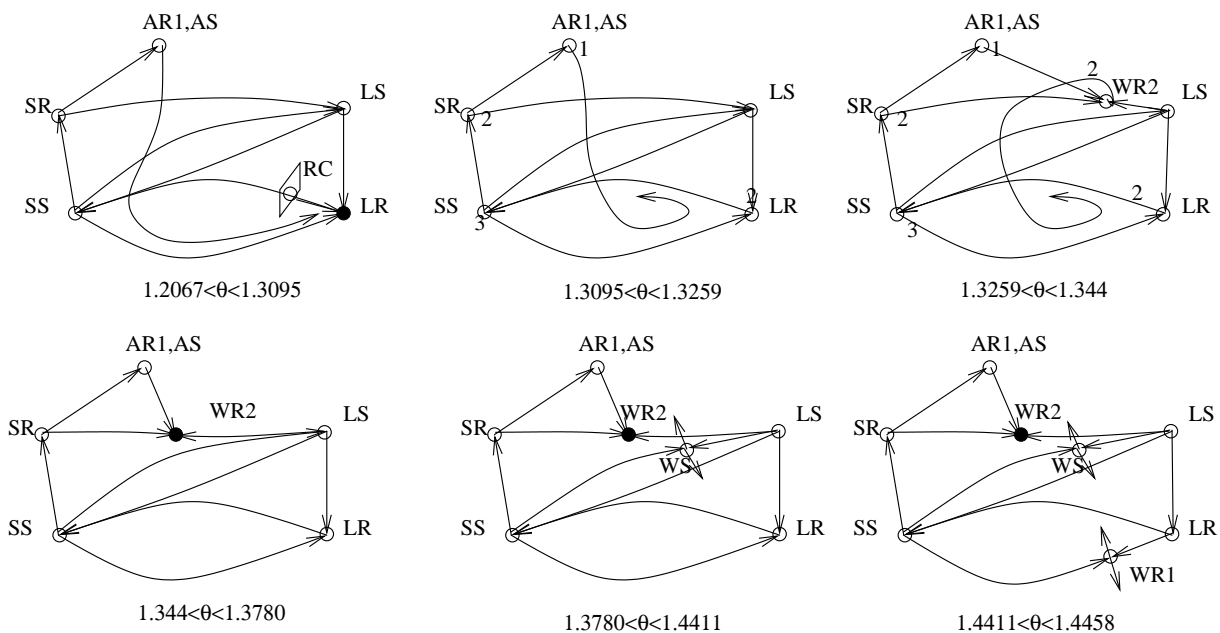
Figure 7: *Schematic illustration of connections between different symmetry types for $P = 1$ between parameters near 18 and 25 of Figure 4(a). Open circles indicate saddles, filled circles are sinks. The size of the unstable manifold (ignoring group orbit directions) is indicated as a number next to that state. Note that for $1.2067 < \theta < 1.3095$ from 12 to 17, LR is the only attractor. For $1.378 < \theta < 1.4411$ from 24 to 26, WR1 is the only attractor. For $1.3095 < \theta < 1.344$ from 17 to 20 the only attractor is a network involving all states and including a connection to the subcycle including LR and SS. The bifurcation at $\theta = 1.344$, 20, is a subcritical Hopf bifurcation that stabilizes the WR2 solution. For $1.344 < \theta < 1.3870$ from 20 to 25 there is still a heteroclinic cycle between LR and SS states but typical orbits near this are transients to the WR2 state.*
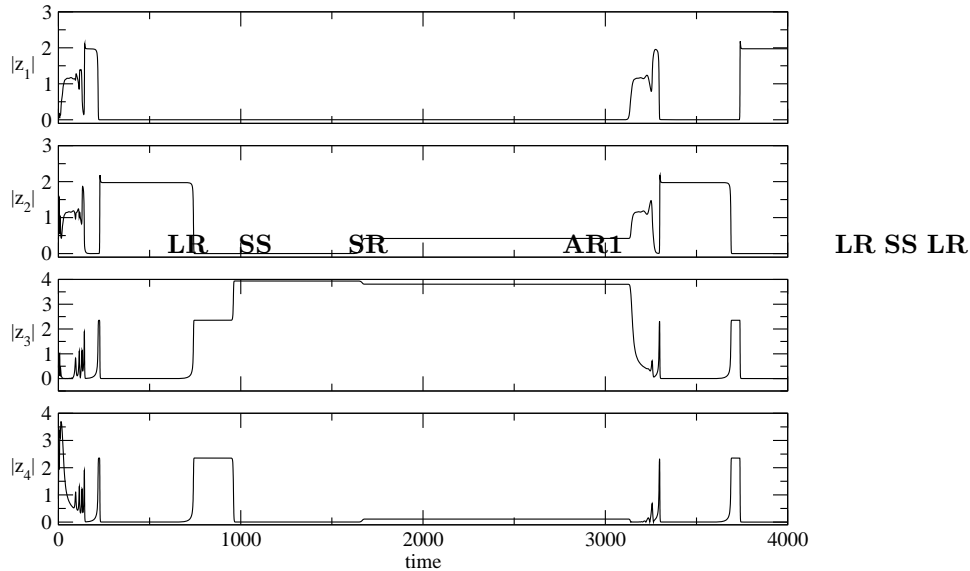
Figure 8: *Time series showing a typical trajectory approaching a depth 2 heteroclinic network for $P = 1$ and $\theta = 1.325$. Note the approach to a cycle between LR and SS states is interrupted by the trajectory choosing the unstable manifold towards an AR1 and then a WR2 state. For $t > 3300$ it heads towards LS before showing oscillatory growth near where WR2 appears for $\theta > 1.3259$.*

(17):

$$\tan \theta = \frac{\lambda_2}{\lambda_1} = \frac{\beta_{21} + \beta_{22}(R - R_m)/\delta}{\beta_{11} + \beta_{12}(R - R_m)/\delta}$$

and hence a straight line on the (k, R) plane corresponds to each value of θ. Therefore, $\theta \to \theta_\infty = \arctan(\beta_{22}/\beta_{12}) \approx 0.900$ as $R \to \infty$ and on the diagrams of Fig. 4 the part $\theta < \theta_\infty$ corresponds to $\delta > 0$ and the part $\theta > \theta_\infty$ to $\delta < 0$.

For $P = 2$ for the range of R where the centre manifold approximation is valid the attractors are either SR or LR, in agreement with results of section 4.1.

For $P = 1$ and $\delta = -0.01k_m$ for increasing R we observe transitions from S_0 to SR and to WR2. Simultaneously with the WR2, there exists another attractor, a periodic orbit of a very large period which is close to the heteroclinic cycle connecting LR and SS. On Figure 9a the plateaux with $|z_1| \neq 0$, $|z_2| \neq 0$ and $|z_3| = |z_4| \neq 0$ indicate time intervals when the shown trajectory is close to large rolls parallel to y-axis, large rolls parallel to x-axis, and to small squares, respectively. The orbit has appeared from the cycle either due to numerical inaccuracy, or perhaps for some other unknown reasons. For larger R the attractor is LR, which then bifurcates to a $\widetilde{\text{TW}}$, this bifurcation being outside the region of validity of the approximation. For $\delta = 0.01k_m$, where the approximation is valid, the attractor is LR.

For $P = 0.5$ and $\delta = -0.01k_m$ we also see bifurcations from S_0 to SR and to WR2. In agreement with the bifurcation diagram for the 8-dimensional system, the periodic orbit bifurcating from WR2 undergoes a saddle-node bifurcation and becomes stable (Figure 9b). Unlike in the 8-dimensional normal form, the branch of periodic orbits ends on the heteroclinic cycle, instead of bifurcating to another orbit (note the similarity between Figures 9a and b; the trajectory visits unstable LR and SS flows on both plots, however the period of the orbit on Figure b is smaller, it increases as R gets closer to the point of bifurcation of the orbit into the heteroclinic cycle involving LR and SS). The bifurcation value of R is the lower end of the interval of chaotic heteroclinic behavior, where trajectories jump between LR and SS steady states. In each run the time spent near each of the steady state changes

25

P	δ	Type of attractor	Interval of existence(R)	Interval of existence(θ)
2	$-0.01k_m$	S_0	$R \leq 681.2$	$\theta \geq 3.1287$
		SR	$681.3 \leq R \leq 736.1$	$0.9549 \leq \theta \leq 3.1068$
		LR	$690.1 \leq R \leq 2200$	$0.9018 \leq \theta \leq 1.3104$
		$\widetilde{TW}$	$R \geq 2300$	$\theta \leq 0.9017$
	$0.01k_m$	S_0	$R \leq 681.0$	$\theta \leq -1.5695$
		LR	$681.1 \leq R \leq 2300$	$-1.5575 \leq \theta \leq 0.8979$
		$\widetilde{TW}$	$R \geq 2400$	$\theta \geq 0.8980$
1	$-0.01k_m$	S_0	$R \leq 681.2$	$\theta \geq 3.1287$
		SR	$681.3 \leq R \leq 687.9$	$1.4762 \leq \theta \leq 3.1068$
		$WR2$	$688 \leq R \leq 689.8$	$1.3275 \leq \theta \leq 1.4661$
		periodic(heteroclinic)	$688.9 \leq R \leq 690.2$	$1.3049 \leq \theta \leq 1.3879$
		LR	$690.3 \leq R \leq 1100$	$0.9069 \leq \theta \leq 1.2996$
		$\widetilde{TW}$	$R \geq 1200$	$\theta \leq 0.9055$
	$0.01k_m$	S_0	$R \leq 681.0$	$\theta \leq -1.5695$
		LR	$681.1 \leq R \leq 1100$	$-1.5575 \leq \theta \leq 0.8920$
		$\widetilde{TW}$	$R \geq 1200$	$\theta \geq 0.8935$
0.5	$-0.01k_m$	S_0	$R \leq 681.2$	$\theta \geq 3.1287$
		SR	$681.3 \leq R \leq 683.2$	$2.5534 \leq \theta \leq 3.1068$
		$WR2$	$683.3 \leq R \leq 687.1$	$1.5697 \leq \theta \leq 2.5190$
		periodic	$686.6 \leq R \leq 687.6$	$1.5084 \leq \theta \leq 1.6421$
		chaotic(heteroclinic)	$687.7 \leq R \leq 688.9$	$1.3879 \leq \theta \leq 1.4973$
		LR	$689 \leq R \leq 800$	$0.9248 \leq \theta \leq 1.3804$
		$\widetilde{TW}$	$R \geq 810$	$\theta \leq 0.9228$
	$0.01k_m$	S_0	$R \leq 681.0$	$\theta \leq -1.5695$
		LR	$681.1 \leq R \leq 780$	$-1.5575 \leq \theta \leq 0.8653$
		$\widetilde{TW}$	$R \geq 790$	$\theta \geq 0.8686$
0.3	$-0.01k_m$	S_0	$R \leq 681.2$	$\theta \geq 3.1287$
		SR	$681.3 \leq R \leq 682.1$	$2.9038 \leq \theta \leq 3.1068$
		$WR2$	$682.2 \leq R \leq 686.4$	$1.6748 \leq \theta \leq 2.8750$
		periodic	$685.9 \leq R \leq 687.4$	$1.5317 \leq \theta \leq 1.7669$
		chaotic(heteroclinic)	$687.5 \leq R \leq 688.1$	$1.4563 \leq \theta \leq 1.5199$
		LR	$688.2 \leq R \leq 720$	$0.9790 \leq \theta \leq 1.4468$
		$\widetilde{PO}$	$R \geq 730$	$\theta \leq 0.9621$
	$0.01k_m$	S_0	$R \leq 681.0$	$\theta \leq -1.5695$
		LR	$681.1 \leq R \leq 710$	$-1.5575 \leq \theta \leq 0.7687$
		$\widetilde{PO}$	$R \geq 720$	$\theta \geq 0.8061$
0.1	$-0.01k_m$	S_0	$R \leq 681.2$	$\theta \geq 3.1287$
		SR	$R = 681.3$	$\theta = 3.1068$
		$WR2$	$681.4 \leq R \leq 686.2$	$1.7097 \leq \theta \leq 3.0841$
		periodic	$685.7 \leq R \leq 686.7$	$1.6266 \leq \theta \leq 1.8084$
		chaotic(heteroclinic)	$686.8 \leq R \leq 687.3$	$1.5440 \leq \theta \leq 1.6117$
		LR	$687.4 \leq R \leq 690$	$1.3159 \leq \theta \leq 1.5317$
		$\widetilde{PO}$	$R \geq 691$	$\theta \leq 1.2660$
	$0.01k_m$	S_0	$R \leq 681.0$	$\theta \leq -1.5695$
		LR	$681.1 \leq R \leq 684$	$-1.5575 \leq \theta \leq -1.0009$
		$\widetilde{PO}$	$R \geq 685$	-0.7087

Table 11: *Attractors found in numerical simulations of convective flows.*

randomly, unlike for $P = 1$ (Figure 9a). We also observe occasional transitions $SS \rightarrow LS \rightarrow SS$ (e.g. the trajectory shown on Figure 9c at $t \approx 8500$ is close to the LS steady state, other plateaux correspond to the LR or SS steady states), i.e. another cycle predicted by the theory persists in the temporal evolution.

For $P = 0.3$ and for $P = 0.1$ attractors are the same as for $P = 0.5$. For $P = 0.1$ the heteroclinic cycle connecting SS and LS is always unstable, but it is visible as a transient in some runs for $687.8 \leq R \leq 688.1$ (on Figure 9d in the interval $1000 \leq t \leq 6500$, when $|z_1|$ and $|z_2|$ are small the trajectory is close to SS, and when $|z_3|$ and $|z_4|$ are small to LS).

In simulations with $\delta = \pm 0.05 k_m$ and $P = 1$ the same sequence of bifurcations as for $\delta = \pm 0.01 k_m$ has been observed. In [18] numerical investigation of convective attractors was carried out with $L = 4$ (i.e. $\delta = -0.16 k_m$) and $P = 6.8, 1$ and 0.3. Some of the observed bifurcations are the same as in the reduced system considered here, but several are different, e.g. for $P = 1$ and 0.3 the bifurcation from WR2 is supercritical.

# 6 Comparison of bifurcations in the original and reduced systems

Critical values of θ for the reduced system and for the original convective system are compared in Table 12 for the bifurcations which are identical in two systems. Since for the convective system results are obtained numerically, information about bifurcations of attractors only is available, and only brackets for critical θ's are known.

The critical values of θ (see Table 12) are similar for the original and reduced systems. Attractors (for R such that the center manifold approximation is valid) are also similar, except where heteroclinic attractors are present. In such cases the numerics may not shadow the true system dynamics. This is because numerical noise (including rounding errors) can cause the heteroclinic attractor to appear as a long period orbit that moves very close to states with different symmetries.

In the convective simulations analogues of the following attractors of the reduced system were not found: for $P = 0.5$ periodic orbits existing between bifurcations *36* and *35*; for $P = 0.3$ periodic orbits existing between *25* and *35*; for $P = 0.1$ the irregular chaotic attractor illustrated in Figure 5 between *25* and *37* is replaced by a more regular heteroclinic behaviour, similar to the one shown on Figures 9a and c.

Hence many of the more subtle effects due to heteroclinic connections within attractors are not well reproduced numerically. Indeed numerical integration of the original system can be viewed as an ideal system perturbed by low-amplitude numerical noise. It is known [23] that additive noise in a system with heteroclinic attractors typically produces approximately periodic behaviour and this is what we often observe. Similarly, an orbit of a very long period instead of a theoreticaly predicted heteroclinic cycle related to the 1 : 2 mode interaction was observed in non-Boussinesq convection by Mercader et al. [15]. They suggested that higher modes present in the PDE's could possibly prevent formation of the structurally stable heteroclinic cycle (or perhaps destabilize it) with the result that a long periodic orbit was present instead.

Center manifold approximation is not valid for the R's for which bifurcations to $\widetilde{TW}$ and $\widetilde{PO}$ (see Table 11) take place ($\widetilde{TW}$ and $\widetilde{PO}$ are periodic in time, and in the system (12) no bifurcations from rolls to time-periodic flows are possible, see Table 3). The range of validity of the approximation decreases with P, for the considered $|\delta| = 0.01 k_m$ it is $(R - R_c) \sim 3.5 R_c$ for $P = 2$ and $(R - R_c) \sim 0.005 R_c$ for $P = 0.01$.
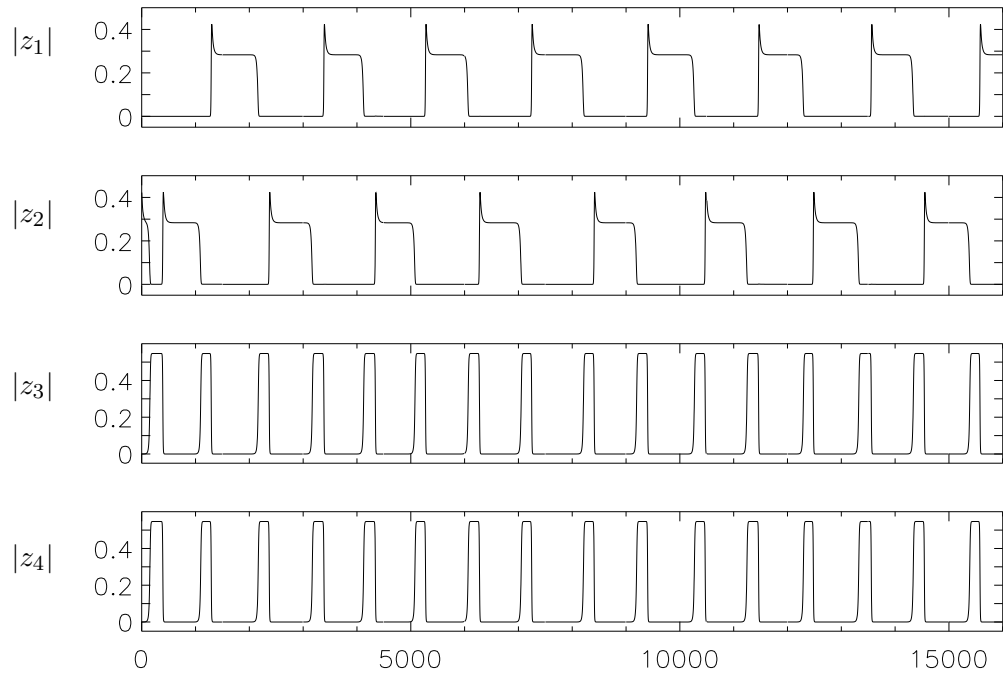
(a)
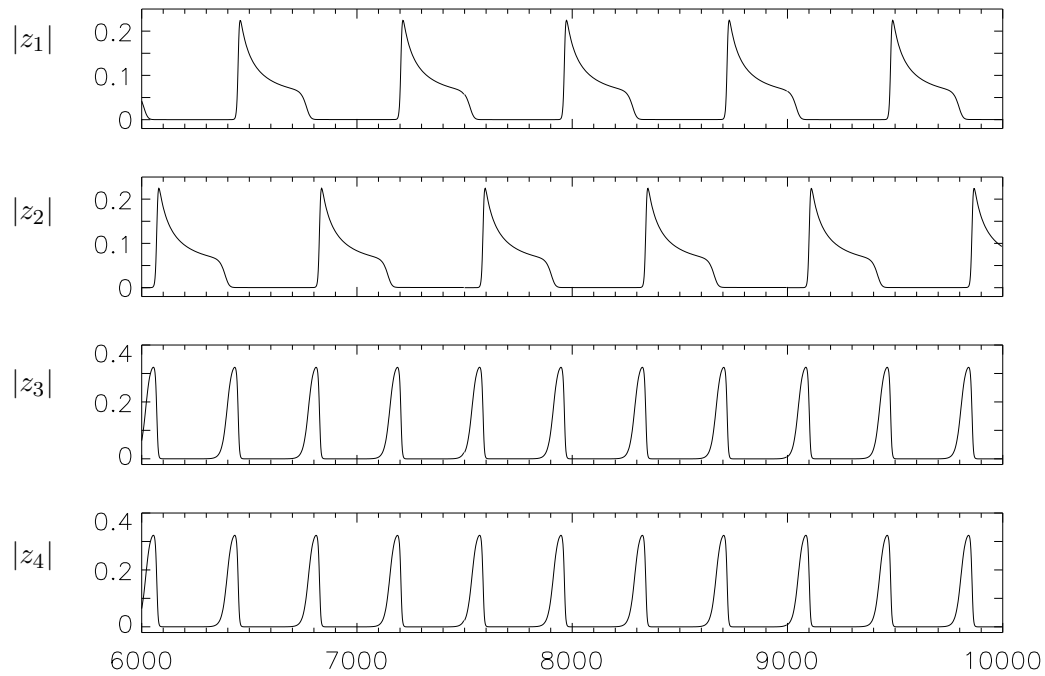
(b)

Figure 9: *Temporal evolution of the quantities $|z_1|$, $|z_2|$, $|z_3|$ and $|z_4|$ of convective attractors for $\delta = -0.01 k_m$ (k = 1.84) and (a) P = 1, R = 690 (θ = 1.3159); (b) P = 0.5, R = 687.5 (θ = 1.5199); (c) P = 0.5, R = 688.5 (θ = 1.4219) and (d) P = 0.1, R = 688 (θ = 1.4661). (See details in the text.) By $|z_i|$, i = 1, 4, we denote projections into the basic vectors in the centre eigenspace. The horizontal axis shows time.*
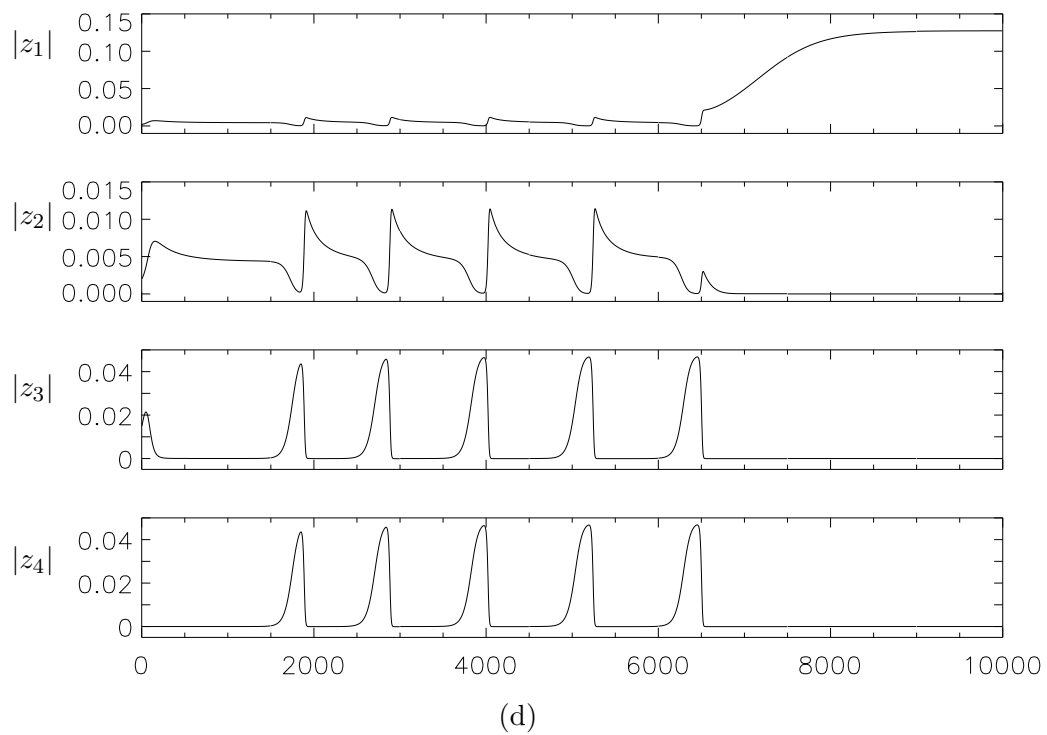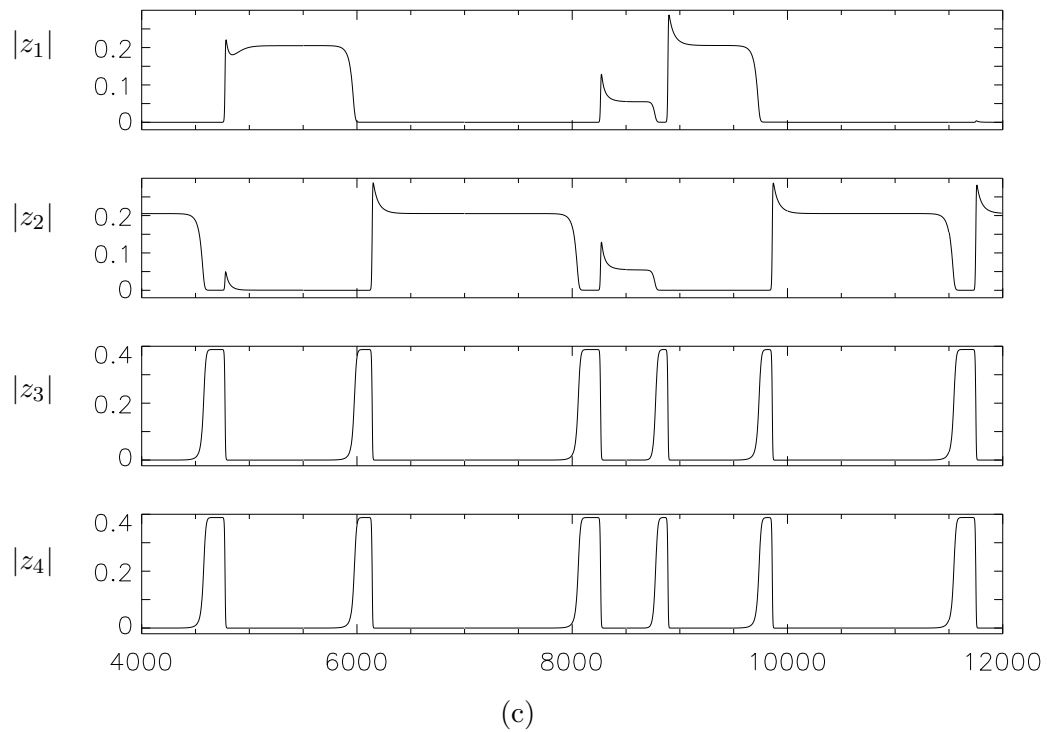
28

(c)

(d)

Figure 9 continued

P	number of bifurcation	θ_c (reduced system)	θ_c (convection)
2	1	$-\pi/2$	$(-1.5695, -1.5575)$
	26	0.89	$(0.9548, 0.9549)$
	17	1.28	$(1.3104, 1.3159)$
	33	π	$(3.1068, 3.1287)$
1	1	$-\pi/2$	$(-1.5695, -1.5575)$
	17	1.3095	$(1.2996, 1.3049)$
	20	1.330	$(1.3216, 1.3275)$
	26	1.4458	$(1.4661, 1.4762)$
	33	π	$(3.1068, 3.1287)$
0.5	1	$-\pi/2$	$(-1.5695, -1.5575)$
	17	1.390	$(1.3804, 1.3879)$
	36	1.500	$(1.4973, 1.5084)$
	20	1.547	$(1.5566, 1.5697)$
	34	1.646	$(1.6421, 1.6581)$
	26	2.557	$(2.5190, 2.5534)$
	33	π	$(3.1068, 3.1287)$
0.3	1	$-\pi/2$	$(-1.5695, -1.5575)$
	17	1.465	$(1.4468, 1.4563)$
	25	1.548	$(1.5199, 1.5317)$
	20	1.625	$(1.6521, 1.6748)$
	34	1.76	$(1.7669, 1.7873)$
	26	2.911	$(2.8750, 2.9038)$
	33	π	$(3.1068, 3.1287)$
0.1	1	$-\pi/2$	$(-1.5695, -1.5575)$
	17	1.553	$(1.5337, 1.5440)$
	25	1.567	$(1.6117, 1.6226)$
	20	1.647	$(1.6920, 1.7097)$
	34	1.85	$(1.8084, 1.8303)$
	26	3.106	$(3.0841, 3.1068)$
	33	π	$(3.1068, 3.1287)$

Table 12: *Comparison of critical values of θ's for bifurcation occurring in the original convection problem and the reduced system.*

7 Conclusions

We have analyzed bifurcations of steady states and travelling waves emerging in the third order normal form invariant under the considered action of $\mathbf{D}_4 \ltimes \mathbf{T}^2 \times \mathbf{Z}_2$ for arbitrary normal form coefficients. We have derived sufficient conditions for existence in the system of up to seven types of distinct (unrelated by symmetries) heteroclinic connections, which can form a complex network. The results have been applied to Boussinesq convection in a plane layer with stress-free boundaries and a square lattice periodicity in horizontal directions. They can be applied to other planar systems, e.g. to Boussinesq convection with other boundary conditions (as long as they are the same on upper and lower boundaries) or to systems in chemistry and biology.

For a complete study of bifurcations of steady states in the system with the symmetry group $\mathbf{D}_4 \ltimes \mathbf{T}^2 \times \mathbf{Z}_2$ some of the fifth order terms should be included into the normal form. They become important if $A_1 = A_2$ or $A_5 = A_6$. However, in Boussinesq convection with both stress-free or both rigid boundaries, these coefficients are unequal and thus the fifth order terms are irrelevant. In Boussinesq binary-fluid convection and magnetoconvection (with the same symmetry groups) with stress-free boundaries these pairs of of normal form coefficients are never equal [21, 5] as well.

For several values of Prandtl number comparison has been carried out between attractors of the reduced system and attractors found by numerical simulation of equations for convection. The attractors are similar in both systems, except for some heteroclinic attractors; this is apparently the effect of numerical noise which is introduced into the convection system [23]. Critical parameter values also turn out to be close as demonstrated in Table 12. The interval where the center manifold approximation is valid varies from $R - R_c < 3.5R_c$ at $P = 2$ to $R - R_c < 0.005R_c$ at $P = 0.1$. For Prandtl number close to $P = 1$ and below the reduced system possesses complex heteroclinic networks. We observe some highly nontrivial intermittent spatio-temporal behavior in the form of heteroclinic cycles of depth 2.

Natural questions arising from this study are what happens if symmetries of the system are slightly broken: square periodicity cell is changed to a rectangular or rhombic cell, weak rotation or weak non-Boussinesq effects are added. In the presence of weak symmetry breaking, heteroclinic attractors are typically destroyed giving rise to temporally periodic intermittent oscillations. It would be interesting to understand the influence of noise on the attracting heteroclinic dynamics, for example that observed in Figure 7. Preliminary investigations indicate that it appears to stabilize the cycle between SS and LR. Finally, the convective regimes that we consider can be unstable to perturbations with other spatial periods. Nonetheless our results give a good indication of minimum complexity of the spatio-temporal dynamics of planar convection.

A Steady state bifurcation with the $\mathbf{D}_2 \ltimes \mathbf{T} \ltimes \mathbf{Z}_4$ symmetry group

We apply theory and methods of [9] to find branches of steady states emerging in a steady state bifurcation with this symmetry group. Consider the action of $\mathbf{D}_2 \ltimes \mathbf{T} \times \mathbf{Z}_4$ on $\mathbf{C}^2$ generated by

$$h_1(= s_2): \ (w_1, w_2) \to (\bar{w}_1, \bar{w}_2),$$

$$h_2(= s_6): \quad (w_1, w_2) \to (w_2, w_1),$$
$$\psi_\alpha(= \gamma_\alpha^{x,-y}): \quad (w_1, w_2) \to (e^{2\pi i\alpha/L} w_1, e^{-2\pi i\alpha/L} w_2),$$
$$h_3(= \gamma_{L/4}^{xy} r): \quad (w_1, w_2) \to (-iw_1, -iw_2).$$

The third order dynamical system commuting with the group action (derived following the procedure described in [19]) is

$$
\begin{aligned}
\dot{w}_1 &= \mu w_1 + w_1(B_1|w_1|^2 + B_2|w_2|^2) + B_3 \bar{w}_1(\bar{w}_2)^2, \\
\dot{w}_2 &= \mu w_2 + w_2(B_1|w_2|^2 + B_2|w_1|^2) + B_3 \bar{w}_2(\bar{w}_1)^2.
\end{aligned}
\tag{18}
$$

One-dimensional fixed point subspaces are: (x, x) (isotropy subgroup is $\mathbf{D}_2$ generated by h_1 and h_2), (x, ix) (isotropy subgroup is $\mathbf{D}_2$ generated by $\psi_{L/4} h_2$ and $h_1 h_2 h_3$), $(x, 0)$ (isotropy subgroup is $\mathbf{D}_2$ generated by h_1 and $h_3 \psi_{L/4}$). Equations for amplitudes of steady states bifurcating from $(w_1, w_2) = \mathbf{0}$ at $\mu = 0$ in the respective subspaces are:

$$
\begin{aligned}
(x, x): &\quad \mu + (B_1 + B_2 + B_3)x^2 = 0, \\
(x, ix): &\quad \mu + (B_1 + B_2 - B_3)x^2 = 0, \\
(x, 0): &\quad \mu + B_1 x^2 = 0.
\end{aligned}
\tag{19}
$$

Stability of a steady state is determined by eigenvalues of Eq. (18) linearized in the vicinity of the steady state, which are:

steady state	eigenspace	eigenvalue
(x, x)	(q, q)	$2(B_1 + B_2 + B_3)x^2$
	$(q, -q)$	$2(B_1 - B_2 - B_3)x^2$
	(iq, iq)	$-4B_3 x^2$
	$(iq, -iq)$	0
(x, ix)	(q, iq)	$2(B_1 + B_2 - B_3)x^2$
	$(q, -iq)$	$2(B_1 - B_2 + B_3)x^2$
	$(iq, -q)$	$4B_3 x^2$
	(iq, q)	0
$(x, 0)$	$(q, 0)$	$2B_1 x^2$
	$(0, q)$	$(-B_1 + B_2 + B_3)x^2$
	$(0, iq)$	$(-B_1 + B_2 - B_3)x^2$
	$(iq, 0)$	0

$$\tag{20}$$

Comparison of Eq. (19) with Eq. (20) implies that just one branch is stable if all the three bifurcate supercritically, the stable branch is the one with the largest amplitude. If there is a branch bifurcating subcritically, all the three are unstable.

B Bifurcations to travelling waves

In this subsection we consider examples of a steady state bifurcation to travelling waves (which is also called relative equilibria in [12]), a pattern which is steady in a co-moving reference frame and periodic in a reference frame at rest. Such bifurcation happens if the isotypic component containing the critical eigenmode also contains an eigenmode responsible for the shift along the group orbit of the bifurcating steady state (the associated eigenvalue is zero).

Expressions in the r.h.s. of Eq. (13) involve angles only in combinations

$$\phi = 2\theta_1 - \theta_3 - \theta_4 \text{ and } \psi = 2\theta_2 - \theta_3 + \theta_4.$$

Assuming $r_3 \neq 0$ and $r_4 \neq 0$, one can rewrite the system Eq. (13) as

$$
\begin{aligned}
\dot{r}_1 &= r_1(\lambda_1 + A_1 r_1^2 + A_2 r_2^2 + A_3(r_3^2 + r_4^2)) + A_4 r_1 r_3 r_4 \cos\phi \\
\dot{r}_2 &= r_2(\lambda_1 + A_1 r_2^2 + A_2 r_1^2 + A_3(r_3^2 + r_4^2)) + A_4 r_2 r_3 r_4 \cos\psi \\
\dot{r}_3 &= r_3(\lambda_2 + A_5 r_3^2 + A_6 r_4^2 + A_7(r_1^2 + r_2^2)) + A_8(r_2^2 r_4 \cos\psi + r_1^2 r_4 \cos\phi) \\
\dot{r}_4 &= r_4(\lambda_2 + A_5 r_4^2 + A_6 r_3^2 + A_7(r_1^2 + r_2^2)) + A_8(r_2^2 r_3 \cos\psi + r_1^2 r_3 \cos\phi) \\
\dot{\phi} &= \sin\phi(-2A_4 r_3 r_4 - A_8 r_1^2(r_4/r_3 + r_3/r_4)) - \sin\psi A_8 r_2^2(r_4/r_3 - r_3/r_4) \\
\dot{\psi} &= \sin\psi(-2A_4 r_3 r_4 - A_8 r_2^2(r_4/r_3 + r_3/r_4)) - \sin\phi A_8 r_1^2(r_4/r_3 - r_3/r_4).
\end{aligned}
\tag{21}
$$

The steady states of Eq. (21) with $\phi = \psi = 0$ are true steady states of Eq. (13). Steady states with one of ϕ or ψ non-vanishing are patterns drifting along the x or y direction, respectively. If $\phi = \pm\psi \neq 0$, the pattern is drifting along the diagonal. Finally, if $0 \neq \phi \neq \psi \neq 0$, there is drift in both horizontal directions.

B.1   Bifurcation from RC

A steady state of Eq. (21) which belongs to the subspace $(r_1, 0, r_3, r_3, \phi, 0)$ satisfies

$$\lambda_1 + A_1 r_1^2 + 2A_3 r_3^2 + A_4 r_3^2 \cos\phi = 0,$$

$$\lambda_2 + (A_5 + A_6) r_3^2 + A_7 r_1^2 + A_8 + r_1^2 \cos\phi = 0,$$

$$A_4 r_3^2 + A_8 r_1^2 = 0.$$

For them, both $\phi = 0$ and $\phi \neq 0$ are possible. Assume that λ's depend on a parameter Q. The two types of steady states coincide at a point where

$$\lambda_1(Q) + A_1 r_1^2 + 2A_3 r_3^2 + A_4 r_3^2 = 0,$$

$$\lambda_2(Q) + (A_5 + A_6) r_3^2 + A_7 r_1^2 + A_8 + r_1^2 = 0,$$

$$A_4 r_3^2 + A_8 r_1^2 = 0.$$

This system of 3 equations in 3 variables (Q, r_1, r_3) is, in general, solvable. The steady state with $\phi = 0$ exists for Q both slightly larger and slightly smaller than the critical value, the steady state with $\phi \neq 0$ exists only at one side of the critical Q, because $\cos\phi \leq 1$. The pattern moves along the x axis with the speed

$$\dot\theta_1 = A_4 r_3 r_4 \sin\phi,$$

small near the point of bifurcation.

B.2   Bifurcation from SQ

In polar coordinates the action of the symmetry group of SQ, $\mathbf{D}_4$, on the subspace $(0, 0, 0, 0, \phi, \psi)$ is generated by

$$s_1 : \ (\phi, \psi) \mapsto (\psi, -\phi) \text{ and}$$

$$s_4 : \ (\phi, \psi) \mapsto (\phi, -\psi).$$

Therefore [9], there are two types of maximal isotropy bifurcating branches: with $\psi = 0$ (or $\phi = 0$) and $\psi = \phi$ (or $\psi = -\phi$). They are: TW2= $(r_1, r_2, r_3, r_3, \phi, 0)$ and TW4= $(r_1, r_1, r_3, r_4, \phi, \phi)$. In the normal form Eq. (21) TW4 bifurcating from SQ will have the form $(r_1, r_1, r_3, r_3, \phi, \phi)$ (i.e. $r_3 = r_4$) because the terms breaking this relation are outside the 3rd order truncation we are considering.

C   Bifurcations from AS1

When calculating stability and bifurcations from tertiary branches we have determined 3-dimensional isotypic components for the actions of the steady states symmetry groups. For one- and two-dimensional subspaces the study is straightforward, the case of three dimensions is more difficult. Here we demonstrate that some results on bifurcations and stability can be obtained without explicit calculation of eigenvalues, considering as an example bifurcations from AS1=(x_1, ix_2, x_3, x_3) with the critical mode belonging to the subspace (q_1, iq_2, q_3, q_3).

The matrix of the restriction of the linearization of (8) onto the subspace is

$$\mathcal{B} = \begin{pmatrix} 2A_1 x_1^2 & 2A_2 x_1 x_2 & (4A_3 + 2A_4) x_1 x_3 \\ 2A_2 x_1 x_2 & 2A_1 x_1^2 & (4A_3 - 2A_4) x_2 x_3 \\ 2(A_7 + A_8) x_1 x_3 & 2(A_7 - A_8) x_1 x_3 & 2(A_5 + A_6) x_3^2 \end{pmatrix}. \tag{22}$$

Its eigenvalues satisfy:

$$\mu_1 \mu_2 \mu_3 = \det\mathcal{B}, \quad \mu_1 + \mu_2 + \mu_3 = \mathrm{tr}\mathcal{B}, \quad \mu_1\mu_2 + \mu_1\mu_3 + \mu_2\mu_3 = \tilde{\mathcal{B}},$$

33

where by $\tilde{\mathcal{B}}$ we denoted the sum of the 3 second order minors of $\mathcal{B}$.

The necessary and sufficient conditions for steady state bifurcations are $\det \mathcal{B} = 0$. Eq. (22) implies that $\det \mathcal{B} = x_1^2 x_2^2 x_3^2 F(\mathbf{A})$. The values of x_j, $j = 1, 2, 3$ for the steady state satisfy a linear system of equations on x_j^2, stemming from (12). By Kramer's rule, the solution of the system is

$$x_j^2 = \frac{g_j(\lambda_1, \lambda_2, \mathbf{A})}{f(\mathbf{A})}, \quad j = 1, 2, 3,$$

where g_j is linear in λ's and quadratic in A's, and f is cubic in A's. It turns out that $f(\mathbf{A}) = F(\mathbf{A})$. Hence, the condition $\det \mathcal{B} = 0$ is never satisfied and the condition $F(\mathbf{A}) = 0$ gives a boundary of the domain where AS1 exists.

A Hopf bifurcation takes place if

$$\mathrm{tr}\mathcal{B}\tilde{\mathcal{B}} = \det \mathcal{B}, \quad \tilde{\mathcal{B}} > 0;$$

hence bifurcations from the steady state can be found by solving this equation simultaneously with equations for the steady state.

D Calculation of λ_1 and λ_2

We calculate here coefficients of the linear terms of (12).

Denote by $\mathcal{L}$ the system Eq. (1)-Eq. (4) linearized near the trivial steady state. The subspace spanned by

$$\mathbf{S}_1 = \begin{pmatrix} -\pi l^{-1} \cos \pi z \sin lx \\ 0 \\ \sin \pi z \cos lx \\ 0 \end{pmatrix}, \mathbf{S}_2 = \begin{pmatrix} 0 \\ \cos \pi z \sin lx \\ 0 \\ 0 \end{pmatrix}, \mathbf{S}_3 = \begin{pmatrix} 0 \\ 0 \\ 0 \\ \sin \pi z \cos lx \end{pmatrix} \tag{23}$$

is $\mathcal{L}$-invariant:

$$\begin{aligned} \mathcal{L}\mathbf{S}_1 &= -Pa\mathbf{S}_1 + \mathbf{S}_3, \\ \mathcal{L}\mathbf{S}_2 &= -Pa\mathbf{S}_2, \\ \mathcal{L}\mathbf{S}_3 &= PRl^2 a^{-1}\mathbf{S}_1 - a\mathbf{S}_3, \end{aligned} \tag{24}$$

where $a = l^2 + \pi^2$. Therefore, there is an eigenvalue $-P(l^2 + \pi^2)$ with the associated eigenvector $\mathbf{S}_2$ and two eigenvalues

$$\Lambda_\pm(l, R) = \frac{1}{2}(-(Pa + a) \pm D^{1/2}) \text{ where } D = (Pa + a)^2 - 4(Pa^2 - PRl^2 a^{-1}).$$

In the vicinity of l_0 and R_0, such that $\Lambda_+(l_0, R_0) = 0$, Taylor expansion of Λ_+ in $\delta = l - l_0$ and $\epsilon = R - R_0$ yields:

$$\Lambda_+(l, R) = P(P + 1)^{-1}(2(\pi^2 - 2l_0^2)l_0^{-1}\delta + l_0^2 a^{-2}\epsilon) + O(\epsilon^2 + \delta^2). \tag{25}$$

Substituting into Eq. (25) $l_0 = k_m$ and $l_0 = \sqrt{2}k_m$, find

$$\lambda_1 = P(P + 1)^{-1}(2(\pi^2 - 2k_m^2)k_m^{-1}\delta + k_m^2(\pi^2 + k_m^2)^{-2}\epsilon) + O(\epsilon^2 + \delta^2)$$

and

$$\lambda_2 = P(P + 1)^{-1}(2(\pi^2 - 4k_m^2)k_m^{-1}\delta + 2k_m^2(\pi^2 + 2k_m^2)^{-2}\epsilon) + O(\epsilon^2 + \delta^2).$$

For k_m given by (8) these relations yield the coefficients β_{ij} presented in Table 9.

E Center manifold reduction

The centre manifold is an invariant manifold tangent to X_c at $(\mathbf{0}, R_m)$; standard theory [11] means that near a bifurcation the local solutions are determined by the dynamics on the centre manifold. Locally it is represented as a graph of the mapping $\psi(\mathbf{v}) : X_c \to X_h$ defined in a neighborhood of $(\mathbf{0}, R_m)$.

The second-order Taylor's expansion is

$$\psi(\mathbf{v}) = \sum_{j,l=1}^{4} \phi_{j,l}^1 x_j x_l + \sum_{j,l=1}^{4} \phi_{j,l}^2 x_j y_l + \sum_{j,l=1}^{4} \phi_{j,l}^3 y_j y_l, \tag{26}$$

34

where x_j and y_l are components of $(\mathbf{v}) \in X_c$ in the basis $\{\mathbf{X}_j, \mathbf{Y}_l\}$ and $\phi \in X_h$.

Denote

$$\mathbf{f}_1(m_1, m_2, m_3) = \begin{pmatrix} k_m m_2 \cos m_3 \pi z \sin(m_1 k_m x + m_2 k_m y) \\ -k_m m_1 \cos m_3 \pi z \sin(m_1 k_m x + m_2 k_m y) \\ 0 \\ 0 \end{pmatrix}, \tag{27}$$

$$\mathbf{f}_2(m_1, m_2, m_3) = \begin{pmatrix} -\pi k_m m_1 m_3 \cos m_3 \pi z \sin(m_1 k_m x + m_2 k_m y) \\ -\pi k_m m_2 m_3 \cos m_3 \pi z \sin(m_1 k_m x + m_2 k_m y) \\ (m_1^2 + m_2^2) k_m^2 \sin m_3 \pi z \cos(m_1 k_m x + m_2 k_m y) \\ 0 \end{pmatrix}, \tag{28}$$

$$\mathbf{f}_3(m_1, m_2, m_3) = \begin{pmatrix} 0 \\ 0 \\ 0 \\ \sin m_3 \pi z \cos(m_1 k_m x + m_2 k_m y) \end{pmatrix}. \tag{29}$$

The center manifold coefficients are:

$$\phi_{1,1}^1 = (8a_1 \pi)^{-1} \mathbf{f}_3(0, 0, 2),$$

$$\phi_{3,3}^1 = (8a_2 \pi)^{-1} \mathbf{f}_3(0, 0, 2),$$

$$\phi_{1,2}^1 = g_1^{-1}((P^{-1}b_1 + b_2)(\mathbf{f}_2(1, 1, 2) + \mathbf{f}_2(1, -1, 2)) + (P^{-1}b_3 + b_4)(\mathbf{f}_3(1, 1, 2) + \mathbf{f}_3(1, -1, 2))),$$

$$\phi_{3,4}^1 = g_2^{-1}((P^{-1}b_5 + b_6)(\mathbf{f}_2(2, 0, 2) + \mathbf{f}_2(0, 2, 2)) + (P^{-1}b_7 + b_8)(\mathbf{f}_3(2, 0, 2) + \mathbf{f}_3(0, 2, 2))),$$

$$\phi_{1,3}^1 = P^{-1}(c_1 \mathbf{f}_1(0, 1, 0) + c_2 \mathbf{f}_1(2, 1, 0) + c_3 \mathbf{f}_1(0, 1, 2) + c_4 \mathbf{f}_1(2, 1, 2) +$$

$$g_3^{-1}((d_1 + Pd_2)\mathbf{f}_2(0, 1, 2) + (d_3 + Pd_4)\mathbf{f}_3(0, 1, 2)) + g_4^{-1}((d_5 + Pd_6)\mathbf{f}_2(2, 1, 2) + (d_7 + Pd_8)\mathbf{f}_3(2, 1, 2))),$$

where

$$a_1 = \pi^2 + k_m^2, \ a_2 = \pi^2 + 2k_m^2, \ a_3 = 2\pi^2 + k_m^2, \ a_4 = 4\pi^2 + k_m^2, \ a_5 = 4\pi^2 + 5k_m^2,$$
$$b_1 = -\pi a_1 (2k_m^2)^{-1}, \ b_2 = -R\pi(4a_1 a_3)^{-1}, \ b_3 = -\pi a_1 (2a_3)^{-1}, \ b_4 = -\pi a_3 a_1^{-1}, \ b_5 = -\pi a_2 (4k_m^2)^{-1},$$
$$b_6 = -R\pi(8a_1 a_2)^{-1}, \ b_7 = -\pi a_2 (4a_1)^{-1}, \ b_8 = -\pi 2a_1 a_2^{-1}$$
$$g_1 = 4a_3^2 - k_m^2 Ra_3^{-1}, \ g_2 = 16a_1^2 - k_m^2 Ra_1^{-1}, \ g_3 = a_4^2 - Rk_m^2 a_4^{-1}, \ g_4 = a_5^2 - 5Rk_m^2 a_5^{-1},$$
$$c_1 = \pi^2 (8k_m^2)^{-1}, \ c_2 = -\pi^2 (200k_m^4)^{-1}, \ c_3 = -\pi^2 (8k_m^2 a_4)^{-1}, \ c_4 = \pi^2 (40k_m^2 a_5)^{-1},$$
$$d_1 = -\pi(7k_m^2 + 4\pi^2)(8k_m^2)^{-1}, \ d_2 = -\pi R((2a_2)^{-1} + 3(8a_1)^{-1})a_4^{-1},$$
$$d_3 = -\pi(7k_m^2 + 4\pi^2)(8a_4)^{-1}, \ d_4 = -\pi a_4((2a_2)^{-1} + 3(8a_1)^{-1}),$$
$$d_5 = -\pi a_5 (40k_m^2)^{-1}, \ d_6 = -\pi R(8a_1 a_5)^{-1}, \ d_7 = -\pi/8, \ d_8 = -\pi a_5 (8a_1)^{-1}.$$

All other coefficients of Eq. (26) can be obtained from these applying symmetries of the system.

F   Exact expressions for the normal form coefficients

$$A_1 = -\frac{1}{8}P(P+1)^{-1},$$

$$A_2 = A_1 - g_1^{-1}(P+1)^{-1}(P^{-1}\frac{1}{2}\pi^2 a_1 + R\pi^2 k_m^2 (a_1(2k_m^2 + 4\pi^2))^{-1} + \frac{1}{4}P\pi^2(2k_m^2 + 4\pi^2)),$$

$$A_3 = -P(P+1)^{-1}a_1(8a_2)^{-1} +$$

$$(P+1)^{-1}k_m^2(8a_1)^{-1}(4c_1 k_m^2 + 2(2\pi^2 - k_m^2)(2c_2 + c_3) + 2c_4 k_m^2 + g_3^{-1}(P^{-1}d_1 + d_2)\pi(5k_m^2 - \pi^2) +$$

$$g_4^{-1}(P^{-1}d_5 + d_6)\pi(7k_m^2 + 5\pi^2)) + P(P+1)^{-1}a_1(8a_2)^{-1}(2k_m^2(2c_1 - 2c_2 - c_3 + c_4) + 2\pi k_m^2 g_3^{-1}(P^{-1}d_1 + d_2) +$$

$$3\pi a_2 g_3^{-1}(P^{-1}d_3 + d_4) + 2\pi k_m^2 g_4^{-1}(P^{-1}d_5 + d_6) + \pi a_2 g_4^{-1}(P^{-1}d_7 + d_8)),$$

$$A_4 = (P+1)^{-1}k_m^2(4a_1)^{-1}(-4c_1 k_m^2 - 2(2\pi^2 - k_m^2)c_3 + g_3^{-1}(P^{-1}d_1 + d_2)\pi(5k_m^2 - \pi^2)) +$$

$$P(P+1)^{-1}a_1(4a_2)^{-1}(2k_m^2(-2c_1 + c_3) + 2\pi k_m^2 g_3^{-1}(P^{-1}d_1 + d_2) + 3\pi a_2 g_3^{-1}(P^{-1}d_3 + d_4)),$$

$$A_5 = A_1,$$

$$A_6 = A_5 - g_2^{-1}(P+1)^{-1}(P^{-1}\frac{1}{2}\pi^2 a_2 + R\pi^2 k_m^2 (a_2(2k_m^2 + 2\pi^2))^{-1} + P\pi^2(k_m^2 + \pi^2)),$$

$$A_7 = -P(P+1)^{-1}a_2(8a_1)^{-1} +$$
$$+\frac{k_m^2(-2c_1 a_2 + (2k_m^2 - 3\pi^2)(2c_2 + c_3) - c_4 a_2 + g_3^{-1}(P^{-1}d_1 + d_2)\pi(2k_m^2 + 5\pi^2) - g_4^{-1}(P^{-1}d_5 + d_6)\pi a_2)}{(P+1)4a_2} +$$
$$\frac{a_2(k_m^2(-2c_1 + 2c_2 + c_3 - c_4) - \pi k_m^2 g_3^{-1}(P^{-1}d_1 + d_2) + 2\pi a_1 g_3^{-1}(P^{-1}d_3 + d_4) - \pi k_m^2 g_4^{-1}(P^{-1}d_5 + d_6))}{P(P+1)4a_1},$$

$$A_8 = (P+1)^{-1}k_m^2(4a_2)^{-1}(2a_2 c_1 + (3\pi^2 - 2k_m^2)c_3 + g_3^{-1}(P^{-1}d_1 + d_2)\pi(2k_m^2 + 5\pi^2)) +$$
$$P(P+1)^{-1}a_2(4a_1)^{-1}(k_m^2(2c_1 - c_3) - \pi k_m^2 g_3^{-1}(P^{-1}d_1 + d_2) + 2\pi a_1 g_3^{-1}(P^{-1}d_3 + d_4)).$$

G   Reduction of the group action

The original system of ODEs Eq. (12) on $\mathbf{C}^4$ have a continuous group symmetry $\mathbf{T}^2$ that means that conventional path following programs fail to work. The normal form Eq. (12) in the form can be reduced by the two dimensional group action as follows, so that the remaining system is nondegenerate and on $\mathbf{C}^3$. We write Eq. (12) as

$$\begin{aligned}\dot{z}_1 &= f_1 \\ \dot{z}_2 &= f_2 \\ \dot{z}_3 &= f_3 \\ \dot{z}_4 &= f_3\end{aligned} \tag{30}$$

and then define

$$a_1 = -\frac{\Im(f_1 \bar{z}_1)}{|z_1|^2}, \quad a_2 = -\frac{\Im(f_2 \bar{z}_2)}{|z_2|^2}.$$

The modified system of equations

$$\begin{aligned}\dot{z}_1 &= f_1 + ia_1 z_1 \\ \dot{z}_2 &= f_2 + ia_2 z_2 \\ \dot{z}_3 &= f_3 + i(a_1 + a_2)z_3 \\ \dot{z}_4 &= f_3 + i(a_1 - a_2)z_4\end{aligned} \tag{31}$$

has solutions that are in one-to-one correspondence with those of Eq. (30). This is because the infinitesimal action of $(e^{i\alpha}z_1, z_2, e^{i\alpha}z_3, e^{i\alpha}z_4)$ is $(i\dot\alpha z_1, 0, i\dot\alpha z_3, i\dot\alpha z_4)$ and the infinitesimal action of $(z_1, e^{i\beta}z_2, e^{i\beta}z_3, e^{-i\beta}z_4)$ is $(0, i\dot\beta z_2, i\dot\beta z_3, -i\dot\beta z_4)$. Hence, for our choice of a_1 and a_2, solutions to Eq. (31) satisfy

$$\Im(\dot{z}_1 \bar{z}_1) = 0, \quad \Im(\dot{z}_2 \bar{z}_2) = 0$$

meaning that effectively we have removed the group orbit drift from the trivial stratum of the orbit space. This means that we can set $\Im(z_1) = \Im(z_2) = 0$ and compute all solutions within this six-dimensional section of the orbit space. Note that the equations transformed this way becomes a system on $\mathbf{R}^6$ on parameterizing by $(x_1, x_2, x_3 + iy_3, x_4 + iy_4)$. Care needs to be taken near solutions where z_1 and/or z_2 are zero as the system is singular on $x_1 = x_2 = 0$.

References

[1] P. Ashwin and M.J. Field. Heteroclinic networks in coupled cell systems. *Arch. Rational Mech. Anal.* **148**, 107–143 (1999).

[2] P. Ashwin and O. Podvigina. Hopf bifurcation with cubic symmetry and instability of ABC flow *Proc. Roy. Soc. London.* **459**, 1801–1827 (2003).

[3] J.P. Boyd. *Chebyshev and Fourier Spectral Methods.* Springer-Verlag, Berlin (1989).

[4] T. Chawanya. Infinitely many attractors in a game dynamics system. *Prog. Theor. Phys.* **95**, 679–684 (1996).

[5] T. Clune and E. Knobloch. Pattern selection in three-dimensional magnetoconvection. *Physica D* **74**, 151–176 (1994).

[6] J.H.P. Dawes The $1 : \sqrt{2}$ Hopf/steady-state mode interaction in three-dimensional magnetoconvection. *Physica D* **139**, 109-136, (2000).

[7] B. Dionne, M. Silber and A.C. Skeldon. Stability Results for Steady, Spatially-Periodic Planforms. *Nonlinearity* **10**, 321–354 (1997).

[8] G.B. Ermentrout. *xppaut* (dynamical systems software). Available from http://www.math.pitt.edu/~bard/bardware/ (2000).

[9] M. Golubitsky, I.N Stewart, and D. Schaeffer. *Singularities and Groups in Bifurcation Theory. Volume 2.* Appl. Math. Sci. **69**, Springer-Verlag, New York, (1988).

[10] P. Hirschberg and E. Knobloch. A robust heteroclinic cycle in an $\mathbf{O}(2) \times \mathbf{Z}_2$ steady-state mode interaction. *Nonlinearity*, **11**, 89–104 (1998).

[11] G. Iooss. *Bifurcation of maps and applications* North-Holland, Amsterdam (1979).

[12] M. Krupa. Bifurcations of relative equilibria. *SIAM J. Math. Anal.*, **21**, 1453–1486 (1990).

[13] M. Krupa and I. Melbourne. Asymptotic stability of heteroclinic cycles in systems with symmetry. *Ergodic Theory Dyn. Syst.*, **15**, 121–148 (1995).

[14] M. Krupa. Robust heteroclinic cycles, *J. Nonlinear Science*, **7**, 129–176 (1997).

[15] I. Mercader, J. Prat and E. Knobloch Robust heteroclinic cycles in two-dimensional Rayleigh-Bénard convection without Boussinesq symmetry, *Int. J. Bif. Chaos*, **12**, 2501-2522 (2002).

[16] O.M. Podvigina. Application of the center manifold theorem for investigation of instability of the ABC flow. *Dynamical Systems*, **21**, 191–208 (2006).

[17] O.M. Podvigina. Magnetic field generation by convective flows in a plane layer. *Eur. Phys. J. B*, **50**, 639–652 (2006).

[18] O.M. Podvigina. Magnetic field generation by convective flows in a plane layer: the dependence on the Prandtl number. Submitted to *GAFD*, (2007).

[19] O.M. Podvigina, P. Ashwin and D.J. Hawker. Modelling instability of ABC flow using a mode interaction between steady and Hopf bifurcations with rotational symmetries of the cube, *Physica D*, **215**, 62-79 (2006).

[20] M.R.E. Proctor and P.C. Matthews. $\sqrt{2} : 1$ Resonance in non-Boussinesq convection. *Physica D* **97**, 229–241 (1996).

[21] M. Silber and E. Knobloch, Pattern selection in steady binary-fluid convection, *Phys. Rev. A*, **38**, 1468–1477 (1988).

[22] M. Silber and E. Knobloch. Hopf bifurcation on a square lattice. *Nonlinearity* **4**, 1063–1107 (1991).

[23] E. Stone and P. Holmes. Random perturbations of heteroclinic attractors. *SIAM J. Appl. Math.* **50**, 726–743 (1990).

[24] J.W. Swift. *Bifurcation and symmetry in convection*, PhD Thesis University of California, Berkeley (1984).